Review

Not peer-reviewed version

A Comprehensive Review of Magnetic Iron Oxide Toxicity Across Animal Models: Mechanistic Insights, Particle-Size Effects, and Implications for Air Pollution Biomonitoring

Oscar Rodolfo Hernández-Montoya , Ana G. Castañeda-Miranda * , Margarita L. Martinez-Fierro * , Rodrigo Castañeda-Miranda , Remberto Sandoval-Aréchiga , Jose R. Gomez-Rodriguez , Héctor Alonso Guerrero-Osuna , Víktor I. Rodríguez-Abdalá , Luis Alberto Flores-Chaires , Salvador Ibarra Delgado

Posted Date: 16 January 2026

doi: 10.20944/preprints202601.1266.v1

Keywords: bioindicator; air particle pollution; *Tillandsia recurvata*; magnetic biomonitoring; green barriers; urban park

Review

A Comprehensive Review of Magnetic Iron Oxide Toxicity Across Animal Models: Mechanistic Insights, Particle-Size Effects, and Implications for Air Pollution Biomonitoring

Oscar Rodolfo Hernández-Montoya [1], Ana G. Castañeda-Miranda [1,*], Margarita L. Martínez-Fierro [2,*], Rodrigo Castañeda-Miranda [3], Remberto Sandoval-Aréchiga [1], Jose R. Gomez-Rodriguez [1], Héctor Alonso Guerrero-Osuna [3], Víktor I. Rodríguez-Abdalá [1], Luis Alberto Flores-Chaires [1] and Salvador Ibarra Delgado [1]

[1] Laboratorio de Magnetismo Ambiental, Posgrado en Ingeniería para la Innovación Tecnológica, Unidad Académica de Ingeniería Eléctrica, Universidad Autónoma de Zacatecas, Zacatecas 98000, Zacatecas, México

[2] Doctorado en Ciencias con Orientación en Medicina Molecular, Unidad Académica de Medicina Humana y Ciencias de la Salud, Universidad Autónoma de Zacatecas, Carretera Zacatecas-Guadalajara Km 6. Ejido la Escondida, Zacatecas 98160, Mexico

[3] Programa en Ingeniería y Tecnología Aplicada. Laboratorio Nacional CONACYT, SEDEAM. Universidad Autónoma de Zacatecas. Av. Ramón López Velarde, Col. Centro 9800, Zacateca, México

* Correspondence: agmiranda@uaz.edu.mx (A.G.C.-M.); margaritamf@uaz.edu.mx (M.L.M.-F.)

Abstract

This study assessed the spatial distribution and composition of airborne particulate matter within a 10-km long urban green corridor in Zacatecas, Mexico, using magnetic biomonitoring with *Tillandsia recurvata* and SEM-EDS particle characterization. A total of 44 samples were collected from distinct urban park contexts (e.g., commercial zones, malls, bus stop), revealing mass-specific magnetic susceptibility χ values ranging from -6.71 to 61.1 × 10^{-8} m^3kg^{-1}. Three compositional groups were identified based on a PCA performed using elemental concentrations from SEM-EDS and magnetic data, which are associated with traffic emissions and industrial inputs. SEM-EDS images confirmed abundant magnetite-like particles (1–8 μm) with hazardous metals including Pb (up to 5.6 wt.%), Ba (up to 67.6 wt.%), and Cr (up to 31.5 wt.%). Wind direction data indicated predominant SSW-NNE transport, correlating with hotspots in central and northeastern park areas. Overall, vegetated zones displayed significantly lower magnetic loads (mean χ = 8.84 × 10^{-8} m^3kg^{-1}, σ = 6.65 × 10^{-8} m^3kg^{-1}) compared to traffic-exposed sites (mean χ = 17.27 × 10^{-8} m^3kg^{-1}, σ = 12.44 × 10^{-8} m^3kg^{-1}), emphasizing the pollution mitigation role of green barriers. This research highlights the applicability of combined magnetic and microscopic techniques for evaluating the dynamics of airborne pollution in urban parks and supports their use as biofunctional filters in cities facing vehicular air pollution.

Keywords: bioindicator; air particle pollution; *Tillandsia recurvata*; magnetic biomonitoring; green barriers; urban park

 doi:10.20944/preprints202601.1266.v1

Graphical Abstract

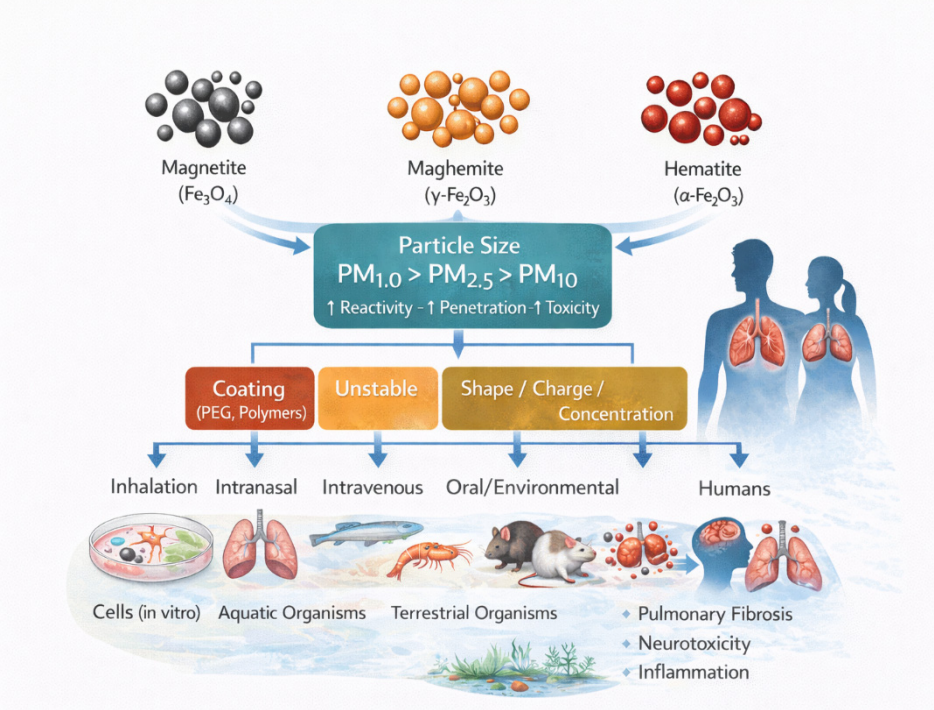

1. Introduction

Iron oxides (IOs) have become among the most extensively investigated transition metal oxides due to their broad range of biomedical and technological applications. However, the rapid expansion of their use has raised increasing concern regarding their potential environmental and human health risks. Iron oxides are naturally occurring minerals composed of iron and oxygen, widely distributed across the Earth's surface and present in multiple crystalline structures. They exhibit diverse physicochemical properties, including optical and thermal stability, superparamagnetic behavior, high chemical reactivity, biodegradability, biocompatibility, and environmental abundance. These properties are strongly governed by particle size, morphology, and specific surface area, which collectively determine their biological and environmental behavior [1,2].

The most common crystalline phases of iron oxides include hematite (α-Fe_2O_3), the thermodynamically most stable and most abundant iron oxide in the biosphere, typically exhibiting a reddish coloration at the nanoscale; maghemite (γ-Fe_2O_3), a metastable iron oxide characterized by ferrimagnetic properties and a brown appearance; and magnetite (Fe_3O_4), commonly referred to as black iron oxide, which displays the strongest magnetic response among transition metal oxides due to its mixed-valence structure [2–4]. The physicochemical properties of IOs can vary substantially depending on particle size, shape, origin, and surface functionalization. In this review, particular attention is given to particulate matter fractions $PM_{1.0}$, $PM_{2.5}$, and PM_{10}, as distinct biological responses have been reported even within the same size class. Such variability has been shown to compromise human health, affect other living organisms, and facilitate the incorporation of iron oxide particles into food webs through multiple exposure pathways [5–8].

Atmospheric particulate matter is commonly classified into coarse particles (PM_{10}), with aerodynamic diameters between 2.5 and 10 μm, including dust, pollen, and mold; fine particles ($PM_{2.5}$), with diameters smaller than 2.5 μm, typically associated with combustion processes and organic compounds; and ultrafine particles or nanoparticles ($PM_{1.0}$), ranging from approximately 1 to 100 nm, which are predominantly generated by coal combustion, metallic emissions, and high-temperature industrial processes [9]. Compared to $PM_{2.5}$ and PM_{10}, $PM_{1.0}$ particles exhibit a markedly higher surface-area-to-volume ratio, increased surface free energy, enhanced surface charge density,

 doi:10.20944/preprints202601.1266.v1

and elevated chemical reactivity, all of which amplify their biological interactions and toxic potential [10,11].

Iron oxide nanoparticles originate from both natural and anthropogenic sources and are continuously introduced into the atmosphere, aquatic systems, and terrestrial ecosystems. Once deposited, they can enter food chains through ingestion or absorption by a wide range of organisms [12]. In urban environments, their abundance has increased substantially due to anthropogenic activities such as fossil fuel combustion, brake and tire wear, steel manufacturing, coal burning, dust storms, wildfires, volcanic activity, vehicular traffic, and other globally distributed industrial processes [13,14]. This growing environmental presence has prompted extensive research into the biological effects of iron oxide nanoparticles, which have been evaluated under diverse experimental frameworks considering particle size, surface coatings, exposure routes, biological models, and intended biomedical or environmental applications [15–21].

Multiple studies have identified iron oxide particles within the $PM_{1.0}$ fraction as posing the highest biological risk, primarily due to their small size, enhanced cellular penetration capacity, and elevated reactivity. Furthermore, the crystalline phase—magnetite, hematite, or maghemite—has been shown to significantly influence the magnitude and nature of toxic responses. Nevertheless, reported effects remain highly variable depending on the biological model, exposure pathway, dose, and experimental conditions. In this context, the objective of the present review is to provide a critical and chronological analysis of the available literature on the biological effects associated with exposure to iron oxide particles. The review systematically differentiates between administration routes, particle size, surface coatings, biological models, and exposure types (acute versus chronic), with the aim of identifying the key physicochemical and biological parameters that govern iron oxide toxicity.

2. Materials and Methods

Experimental studies evaluating the biological effects of iron oxides corresponding to magnetite (Fe_3O_4), hematite (α-Fe_2O_3), and maghemite (γ-Fe_2O_3) were included in this review. For comparative purposes, iron oxide particles were classified within particulate matter size categories $PM_{1.0}$, $PM_{2.5}$, and PM_{10} when this information was explicitly reported or could be reasonably inferred from the physicochemical characterization provided in each study. Studies conducted in animal biological models were considered, including in vivo, in vitro, and ex vivo investigations, as well as a wide range of exposure routes, such as inhalation, intratracheal instillation, oral, dermal, intravenous, intraperitoneal, and aquatic or environmental exposure. Only original research articles published in English were included, primarily covering the period from 2000 to 2025. Nevertheless, earlier studies were incorporated when deemed relevant from a historical, methodological, or toxicological perspective, particularly in the context of chronic occupational exposure or pioneering investigations that remain highly cited.

Exclusion criteria comprised studies evaluating iron-containing materials other than the selected iron oxides, elemental iron, or soluble iron salts (e.g., $FeCl_3$). In addition, review articles, doctoral theses, studies lacking an experimental biological model, investigations focused exclusively on therapeutic or biomedical applications (e.g., magnetic hyperthermia, drug delivery systems, or clinical imaging), and studies lacking essential results or critical methodological information were excluded. Research conducted in non-animal models was likewise not considered. The bibliographic search was performed using PubMed/MEDLINE, Scopus, Web of Science, ScienceDirect, SpringerLink, and Wiley Online Library. Google Scholar was used as a complementary search engine to identify additional non-indexed literature. The final search was conducted on 22 August 2025, using combinations of keywords including iron oxide nanoparticles, magnetite, hematite, maghemite, toxicity, damage, and biological model.

Study selection was performed in two stages. Initially, titles and abstracts were screened to exclude articles that did not meet the predefined inclusion criteria. Subsequently, a full-text assessment of the preselected articles was conducted to confirm eligibility. The entire screening and

 doi:10.20944/preprints202601.1266.v1

selection process was carried out by a single author.From each included study, the following variables were systematically extracted: particle type, particle size, concentration, route of administration, exposure duration, biological model, observed effects, and principal findings. The extracted data were organized according to particle type and biological model, and comparative tables were constructed to systematize the information and facilitate critical analysis. Data management was performed using Microsoft Excel spreadsheets.

This review was conducted using a narrative–critical approach rather than as a quantitative systematic review. Consequently, standardized tools for formal risk-of-bias assessment were not applied, and no statistical or sensitivity analyses were performed. Study quality was evaluated through comparative and critical discussion of the available evidence, considering the experimental variables described above. Accordingly, findings were synthesized qualitatively and descriptively, highlighting the presence or absence of toxic effects and their relationships with particle size, exposure route, and biological model. When specific information was unavailable, data were reported as "not reported". Finally, it is acknowledged that the risk of bias across the analyzed studies is difficult to establish with precision due to substantial methodological heterogeneity, the frequent use of laboratory-engineered particles, and their limited representativeness of particles generated under natural or anthropogenic environmental conditions. In this context, the overall certainty of the compiled evidence is considered low to moderate, underscoring the need to standardize experimental designs and strengthen future studies to obtain more comparable and generalizable results.

3. Results

3.1. Iron Oxides and Biological Damage Across Animal Models

Historically, numerous studies have investigated the biological effects of iron oxide particles without explicitly specifying the crystalline phase involved. Although the specific iron oxide type can often be inferred from the chemical formulation or source material, such assumptions were intentionally avoided in the present review. Instead, results are presented and discussed by differentiating exposure route, particle size, and biological model, irrespective of incomplete phase identification. A summary of the analyzed data is provided in Tables 1 and 2.

3.1.1. Rats

Rats represent one of the most widely used animal models in experimental sciences. In this context, toxic damage induced by 10 nm iron oxide nanoparticles administered intravenously at a dose of 50 mg/kg body weight has been evaluated in Sprague–Dawley rats. Magnetic resonance imaging (MRI) was performed one hour post-administration, and animals were sacrificed 72 h after exposure. The results demonstrated that 10 nm nanoparticles penetrated brain tissue, which was associated with a significant reduction in T_2 relaxation values. Particle retention within brain tissue was observed, indicating translocation from cerebral vasculature to the brain ventricles. These findings were accompanied by a significant reduction in striatal dopamine levels and its metabolites, as well as neuropathological alterations involving neuronal cell bodies, dopaminergic terminals, and cerebral vasculature [22].

In a complementary experimental study, transgenic TgF344-AD rats and wild-type (WT) rats of both sexes were exposed from approximately postnatal day 28 to traffic-related air pollution (TRAP) or filtered air (FA) for extended periods, with evaluations conducted at 3, 6, 10, and 15 months of age. TRAP exposure was carried out continuously in real time using air drawn directly from a traffic tunnel with mixed light- and heavy-duty vehicle flow, whereas control animals were exposed to purified ambient air. The deposition of refractory particles in the brain was assessed using hyperspectral imaging, together with behavioral, biochemical, and histopathological analyses. Animals exposed to TRAP exhibited higher brain particle burdens, accompanied by behavioral alterations and neuropathological features consistent with Alzheimer's disease phenotypes,

 doi:10.20944/preprints202601.1266.v1

including β-amyloid accumulation, increased phosphorylated tau (PHF1), and glial activation. These effects were shown to be dependent on age, sex, and genotype [23].

3.1.2. Cellular Models

Multiple in vitro studies have investigated the neurobiological effects of iron and iron oxide nanoparticles (Fe-NPs/IONs) using neuronal and endothelial cellular models. In human SH-SY5Y neuronal cells, 24 h exposure to spherical Fe-NPs of 10 and 30 nm at concentrations ranging from 2.5 to 10 μg/mL was associated with marked dopaminergic dysfunction, evidenced by significant reductions in intracellular dopamine content (−68% for 10 nm and −52% for 30 nm at 10 μg/mL). These effects were accompanied by increased α-synuclein expression and activation of oxidative stress-related pathways, including c-Abl/phospho-c-Abl signaling. Dose-dependent increases in reactive oxygen species, mitochondrial dysfunction, inhibition of cell proliferation, and activation of pro-apoptotic pathways were also observed. In parallel, an in vitro blood–brain barrier model based on rat brain microvascular endothelial cells (rBMVECs) showed that 24 h exposure to Fe-NPs induced increased ROS production and functional impairment of barrier integrity, as demonstrated by enhanced fluorescein efflux and altered transendothelial electrical resistance (TEER) values [22].

Subsequent studies using human primary fibroblasts (HF) and human glioblastoma cells (U251) evaluated the cytotoxic, genotoxic, and oxidative effects of bovine serum albumin-coated iron oxide nanoparticles with sizes of 85 ± 10 nm, 36 ± 6 nm, and 38 ± 6 nm following direct exposure for 24 and 48 h. No cytotoxic effects were detected after 24 h; however, at 48 h, cytotoxicity became evident, characterized by reduced cell viability, increased ROS generation, and DNA fragmentation assessed by comet assay, reaching up to 23% at the highest dose. In contrast, PEG-coated nanoparticles of 38 ± 6 nm did not induce detectable toxic effects [24]. Finally, murine N13 microglial cells were employed to assess the cytotoxicity of PEG-coated iron oxide nanoparticles with different sizes and morphologies, including spherical particles of 3 and 14 nm and cubic particles of 19–20 nm. Following 24 h exposure to concentrations ranging from 0.1 to 100 μg/mL, no significant reduction in cell viability was observed, indicating good biocompatibility of these nanoparticles in murine in vitro models [25].

3.1.3. Humans

Bourgkard et al. evaluated the association between occupational exposure to iron oxides and lung cancer mortality in workers from a carbon steel manufacturing plant with at least one year of employment. The longitudinal follow-up (1968–1998) included 17,701 individuals. Despite inhaled dust containing 10–50% iron oxides, no significant association with lung cancer risk was observed. In contrast, a significant increase in bladder cancer mortality was identified in relation to oil mist exposure, displaying a clear dose–response relationship [26].

3.1.4. Mice

Mouse models have been extensively used to investigate the systemic and organ-specific effects of iron-containing particulate matter. In a murine model, Marchini et al. evaluated cardiovascular effects following acute exposure to residual oil fly ash (ROFA), a complex environmental particulate material rich in metals, including iron. Particles with a mean aerodynamic diameter of 2.06 ± 1.57 μm were administered intranasally to female Swiss mice at a single dose of 1.0 mg/kg body weight. A significant reduction in cardiac oxygen consumption was observed at 1 and 3 h post-exposure, accompanied by mitochondrial alterations, including impaired state 3 and state 4 respiration, inhibition of respiratory chain complex II, depolarization of mitochondrial membrane potential, and a marked decrease in ATP production [27]. Subsequent investigations expanded the analysis to systemic and pulmonary responses. Increased lipid peroxidation, evidenced by elevated TBARS levels, was observed primarily at 1 and 3 h post-exposure, while protein oxidation increased from 3 h onward, reaching approximately 16% at 5 h. These effects were accompanied by systemic redox

 doi:10.20944/preprints202601.1266.v1

imbalance, characterized by decreased GSH, increased GSSG, and reduced vitamin C levels. Temporal modulation of SOD activity and sustained increases in pro-inflammatory cytokines (TNF-α and IL-6), together with polymorphonuclear leukocyte activation, indicated the establishment of a systemic inflammatory response following particulate matter exposure [28].

In another study, Radu et al. evaluated pulmonary oxidative and inflammatory responses in male CD-1 mice (12–14 weeks old) following exposure to iron oxide nanoparticles encapsulated in phospholipid polymeric micelles (DSPE-PEG). The average particle size of the micelle-encapsulated iron oxide nanoparticles (IONPs-PM) was approximately 21.5 nm. Nanoparticles were administered intravenously via the tail vein at doses of 5 and 15 mg Fe/kg body weight, and biological parameters were assessed at 2, 3, 7, and 14 days post-exposure. Alterations were observed in the activities of key antioxidant enzymes, including catalase (CAT), superoxide dismutase (SOD), glutathione peroxidase (GPx), and glutathione reductase (GR), together with a sustained depletion of reduced glutathione (GSH). Increased levels of malondialdehyde (MDA) and protein carbonyls were detected, along with a reduction in lactate dehydrogenase (LDH) activity, particularly at days 3 and 7, followed by partial recovery by day 14. In addition, pro-apoptotic signaling was evidenced by increased Bax expression, active caspase-3, and TNF-α, accompanied by decreased Bcl-2 levels, with more pronounced effects at the higher dose. Histopathological analysis revealed dose-dependent pulmonary lesions, including inflammatory cell infiltration, thickening of alveolar walls, and collapse of terminal bronchioles [29].

Gestational exposure to iron oxide nanoparticles has also been shown to induce adverse developmental and reproductive effects. In pregnant CD-1 mice, a single intraperitoneal administration of Fe_2O_3 nanoparticles coated with polyethyleneimine (positively charged, ~28 nm) or polyacrylic acid (negatively charged, ~30 nm) was performed on gestational days 8, 9, or 10 at doses of 10 or 100 mg/kg. No significant maternal or fetal effects were observed at the lower dose. In contrast, the higher dose induced surface charge- and timing-dependent toxicity, with a significant increase in fetal loss, particularly following exposure to positively charged nanoparticles on gestational day 10, where resorption rates approached 42%. Moreover, offspring exposed in utero exhibited persistent reproductive alterations in adulthood, including endometrial hyperplasia in females and germ cell loss in male testes. Increased fetal loss was also observed in second-generation crosses, even in the absence of further nanoparticle exposure. Collectively, these findings demonstrate that gestational exposure to iron oxide nanoparticles—especially positively charged formulations—can induce long-lasting and transgenerational adverse effects on reproductive health [30]. In contrast, Caro et al. investigated the in vivo behavior and acute toxicity of PEGylated iron oxide nanoparticles in Balb/c mice. Cubic nanoparticles with an approximate size of 20 nm were administered intravenously via the tail vein at a dose of 5 mg Fe/kg. Magnetic resonance imaging revealed rapid hepatic uptake and early systemic signal enhancement, indicating effective circulation of the contrast agent. Histological analyses showed no detectable alterations in liver or kidney tissues, and body weight remained stable throughout the observation period, indicating the absence of acute toxicity following intravenous administration of these PEGylated nanoparticles, thereby supporting their biocompatibility under the tested conditions [25].

Finally, Dos Santos et al. evaluated the toxicological effects of industrial iron oxide-rich particulate matter originating from an iron ore pelletizing process, without specification of crystalline phase or particle morphology. Environmental characterization identified predominance of PM_{10} and $PM_{2.5}$ fractions, with coarse particles being more abundant. Wild-type (WT) mice and genetically modified mice with reduced vesicular acetylcholine transporter expression (VAChT KD) were exposed under three environmental conditions: vivarium (control), an indoor pelletizing facility, and an urban area located 3.21 miles from the industrial source. Exposure occurred via passive inhalation of contaminated ambient air for approximately two weeks during both summer and winter seasons, under real atmospheric pollution conditions. Measured PM_{10} concentrations ranged from approximately 33 to 164 $\mu g/m^3$, depending on location and season. Exposure to iron-rich dust induced pulmonary inflammation, which was markedly exacerbated in cholinergic-deficient animals, as evidenced by increased airway hyperresponsiveness, inflammation, oxidative stress, and tissue

 doi:10.20944/preprints202601.1266.v1

remodeling. These findings suggest that reduced cholinergic signaling aggravates iron-rich particulate matter-induced pulmonary inflammation, whereas an intact cholinergic system exerts a protective effect against air pollution-related damage [31].

3.1.5. Fish

Among aquatic vertebrate models, zebrafish (Danio rerio) has been increasingly employed to assess nanoparticle toxicity; however, relatively few studies have systematically evaluated in vivo effects of iron oxide nanoparticles. In the study considered here, zebrafish embryos were exposed to PEGylated magnetic iron oxide nanoparticles and manganese ferrite nanoparticles with sizes ranging from 3 to 20 nm at concentrations of 0.01, 0.1, 1, 10, and 100 μg/mL for 24, 48, 72, and 144 h post-fertilization (hpf). Exposure to iron oxide nanoparticles did not induce mortality, malformations, or alterations in hatching rates at any tested concentration, with survival remaining close to 100% up to 6 days post-fertilization, indicating high in vivo biocompatibility. In contrast, manganese-based nanoparticles exhibited clear dose-dependent toxicity, with high mortality observed at 100 μg/mL after 6 days post-fertilization. Notably, all nanoparticle types promoted accelerated hatching at 48 hpf, suggesting that surface coating, concentration, and exposure duration play critical roles in embryonic development [25].

3.1.6. Amphibians

Evidence regarding iron oxide nanoparticle exposure in amphibian models remains scarce. In tadpoles of Duttaphrynus melanostictus, commercially available iron oxide nanoparticles (IONPs) with reported sizes of 20–40 nm and unspecified morphology were evaluated in an aquatic system at concentrations of 5, 10, and 50 mg/L over a 30-day exposure period. Exposure resulted in increased iron bioaccumulation in blood, liver, and kidney tissues, accompanied by hematological alterations affecting red blood cell count, hematocrit, hemoglobin, and erythrocyte indices, as well as lymphocyte levels. In addition, elevated oxidative stress biomarkers and marked reductions in antioxidant enzyme activity were observed, with SOD activity decreasing by approximately 3.6-fold and CAT activity by 6.7-fold relative to controls. Morphological abnormalities were reported at concentrations of 10 and 50 mg/L, whereas no morphological effects were observed at 5 mg/L [32].

Table 1. Biological effects of iron oxide–containing particulate matter across animal models.

Reference	Biological Model	Exposure Route / Particle Type	Main Biological Effects Observed
Imam et al., 2015	Sprague–Dawley rat	Intravenous injection (10 nm iron oxide NPs)	Brain penetration and retention; decreased T_2 relaxation values; reduced striatal dopamine levels; neuronal, dopaminergic, and cerebral vascular damage
Patten et al., 2021	TgF344-AD and WT rats (♂/♀)	Chronic inhalation of traffic-related air pollution (TRAP)	Increased cerebral particle burden; behavioral impairments; Alzheimer-like phenotype (↑β-amyloid, ↑phosphorylated tau, glial activation), dependent on age, sex, and genotype
Marchini et al., 2013	Female Swiss mouse	Intranasal instillation (ROFA, 1 mg/kg)	Reduced cardiac oxygen consumption; mitochondrial dysfunction; decreased ATP production
Marchini et al., 2014	Female Swiss mouse	Intranasal instillation (ROFA)	Systemic oxidative damage; redox imbalance (↓GSH, ↑GSSG); systemic inflammatory response (↑TNF-α, ↑IL-6)
Radu et al., 2015	Male CD-1 mouse	Intravenous injection (IONPs–PM, 5–15 mg Fe/kg)	Pulmonary oxidative stress; activation of apoptotic pathways; dose-dependent lung injury
Di Bona et al., 2015	Pregnant CD-1 mouse	Intraperitoneal injection (Fe_2O_3 nanoparticles)	Fetal loss; surface charge–dependent reproductive toxicity; transgenerational effects

 doi:10.20944/preprints202601.1266.v1

Caro et al., 2019	Balb/c mouse	Intravenous injection (PEGylated iron oxide NPs)	Rapid hepatic uptake without histopathological damage; absence of acute systemic toxicity
Dos Santos et al., 2024	WT and VAChT KD mice	Passive environmental inhalation (iron-rich PM_{10}/$PM_{2.5}$)	Pulmonary inflammation; airway hyperresponsiveness; oxidative stress; exacerbated effects under cholinergic deficiency

Overall, the studies summarized in Table 1 demonstrate that the biological effects associated with iron oxide exposure are strongly dependent on the biological model, exposure route, and particle physicochemical properties. In murine models, systemic administration (intravenous or intraperitoneal) is primarily associated with brain, pulmonary, and hepatic biodistribution, accompanied by oxidative, inflammatory, and apoptotic alterations. In contrast, inhalation or intranasal exposure more accurately reflects environmentally relevant scenarios, inducing dose- and time-dependent pulmonary, cardiovascular, and neurological responses. Importantly, toxicity is not uniform, ranging from the absence of detectable histopathological effects in PEGylated nanoparticles designed for biomedical use to pronounced systemic oxidative damage, mitochondrial dysfunction, neurodegenerative alterations, and transgenerational reproductive effects under environmental or occupational exposure conditions. In this context, organismal physiological status, genetic background, and the integrity of regulatory systems—such as cholinergic signaling—emerge as critical modulators of biological responses to iron oxide–rich particulate matter.

Table 2. In vitro cellular effects of iron oxide nanoparticles.

Reference	Cell Model	Exposure Conditions	Main Cellular Effects Observed
Imam et al., 2015	Human neuronal cells (SH-SY5Y)	Direct exposure (10–30 nm; 2.5–10 μg/mL, 24 h)	Dopaminergic dysfunction; increased ROS production; mitochondrial impairment; activation of pro-apoptotic pathways
Imam et al., 2015	Rat brain microvascular endothelial cells (rBMVECs)	Direct exposure (24 h)	Increased ROS levels; reduced transendothelial electrical resistance (TEER); increased permeability; functional impairment of the blood–brain barrier
Abakumov et al., 2018	Human fibroblasts (HF) and glioblastoma cells (U251)	Direct exposure (24–48 h)	Size- and time-dependent cytotoxicity and genotoxicity; increased ROS generation; DNA fragmentation
Caro et al., 2019	Murine microglial cells (N13)	Direct exposure (0.1–100 μg/mL, 24 h)	No detectable cytotoxicity; preserved cell viability; high biocompatibility

Collectively, in vitro studies indicate that iron and iron oxide nanoparticles induce cell-type–specific responses that depend on particle size, surface properties, and exposure conditions. In human neuronal models (SH-SY5Y), direct exposure is associated with dopaminergic dysfunction, increased oxidative stress, mitochondrial impairment, and activation of pro-apoptotic pathways, suggesting a direct impact on mechanisms relevant to neurodegeneration. Consistently, in blood–brain barrier endothelial models (rBMVECs), nanoparticles compromise barrier integrity, as evidenced by elevated reactive oxygen species, reduced transendothelial electrical resistance, and increased permeability. Cytotoxic and genotoxic effects observed in human fibroblasts and glioblastoma cells further demonstrate a clear dependence on particle size, surface coating, and exposure duration, whereas PEGylated formulations exhibit improved biocompatibility. Finally, the absence of acute cytotoxicity in murine N13 microglial cells reinforces that cellular responses to iron oxide nanoparticles are not uniform but are strongly modulated by physicochemical properties and cell type.

Collectively, in vitro studies indicate that iron and iron oxide nanoparticles induce cell-type–specific responses that depend on particle size, surface properties, and exposure conditions. In human neuronal models (SH-SY5Y), direct exposure is associated with dopaminergic dysfunction, increased oxidative stress, mitochondrial impairment, and activation of pro-apoptotic pathways,

 doi:10.20944/preprints202601.1266.v1

suggesting a direct impact on mechanisms relevant to neurodegeneration. Consistently, in blood–brain barrier endothelial models (rBMVECs), nanoparticles compromise barrier integrity, as evidenced by elevated reactive oxygen species, reduced transendothelial electrical resistance, and increased permeability. Cytotoxic and genotoxic effects observed in human fibroblasts and glioblastoma cells further demonstrate a clear dependence on particle size, surface coating, and exposure duration, whereas PEGylated formulations exhibit improved biocompatibility. Finally, the absence of acute cytotoxicity in murine N13 microglial cells reinforces that cellular responses to iron oxide nanoparticles are not uniform but are strongly modulated by physicochemical properties and cell type.

3.2. Magnetite and Damage Induced in Biological Models

Magnetite (Fe_3O_4) is one of the most common iron oxides, occurring naturally and as a result of anthropogenic activities. It is widely distributed in igneous rocks, soils, sediments, and industrial emissions. Due to its mixed Fe^{2+}/Fe^{3+} structure, magnetite exhibits high electrical conductivity and magnetic properties, which support its extensive technological, biomedical, and environmental applications. In biological and ecotoxicological contexts, magnetite has attracted increasing attention because of its potential to induce adverse effects. In this section, toxicological evidence obtained across different biological models is summarized, with emphasis on particle size, dose, exposure route, and dominant mechanisms (Tables 3 and 4).

3.2.1. Rats

One of the earliest studies evaluating pulmonary toxicity of magnetite was conducted by Pauluhn using *Rattus norvegicus* exposed to magnetite particles by nose-only inhalation. Pigment-grade Fe_3O_4 particles (300–600 nm) were administered over 4 weeks, followed by post-exposure observation periods of up to 6 months, at concentrations ranging from 10.1 to 95.8 mg/m^3. A clear dose-dependent relationship was observed between inhaled concentration and pulmonary particle accumulation, with a marked reduction in lung clearance above ~30 mg/m^3. Inflammatory responses, characterized by increased neutrophils, lactate dehydrogenase (LDH), and total protein in bronchoalveolar lavage, were reported mainly at concentrations ≥50 mg/m^3. These findings indicated that magnetite-induced pulmonary toxicity is closely associated with lung particle burden and saturation of clearance mechanisms, with an inflammatory threshold near 1 mg of retained particles per lung [33].

In a subsequent inhalation study, Pauluhn evaluated pigment-sized magnetite (Fe_3O_4; Ferroxide® black 88P) in Wistar rats following OECD TG#413 guidelines. Animals were exposed for 13 weeks at concentrations of 0, 4.7, 16.6, and 52.1 mg/m^3. Neutrophilia in bronchoalveolar lavage was identified as the most sensitive endpoint, together with inflammatory changes in the upper and lower respiratory tract. Increased lung and lung-associated lymph node weights, collagen fiber accumulation, and particle translocation to lymph nodes were observed at higher doses. An empirical NOAEL of 4.7 mg/m^3 (BMCL 4.4 mg/m^3) was established, supporting a time-adjusted chronic occupational exposure limit of 2 mg/m^3 (alveolar fraction) [34].

Using intratracheal instillation, Szalay et al. reported that spherical magnetite nanoparticles (<50 nm) administered to Wistar rats at doses of 1 and 5 mg/kg induced reduced body-weight gain and focal interstitial inflammation, with mild pulmonary fibrosis detected after 30 days, while no relevant histopathological alterations were observed in other organs [35]. Similarly, Tada et al. demonstrated that single intratracheal instillation of smaller magnetite nanoparticles (5–15 nm) in Fischer 344 rats induced dose-dependent pulmonary inflammation, granuloma formation, macrophage accumulation, and particle deposition in paratracheal lymph nodes, indicating an acute inflammatory response dependent on particle load and size [18].

Systemic exposure studies further revealed prolonged tissue retention of magnetite nanoparticles. Jarockyte et al. reported slow, dose-dependent clearance of oleate-coated superparamagnetic Fe_3O_4 nanoparticles following intramuscular injection in Wistar rats, with

 doi:10.20944/preprints202601.1266.v1

incomplete elimination observed at higher doses even after two months [36]. In addition, Matusiak et al. demonstrated that intravenous administration of low doses of PEG-coated iron oxide nanoparticles induced transient but significant alterations in hepatic elemental composition, including persistent changes in Ca, Cu, and Zn levels, despite the absence of marked systemic toxicity [37].

3.2.2. Cell Models

In vitro studies consistently demonstrate that magnetite particles of different sizes are internalized by cells, primarily via endocytosis. In human lung epithelial A549 cells, Könczöl et al. showed that bulk, respirable, alveolar, and nanoscale magnetite particles induced oxidative stress, mitochondrial membrane potential alterations, DNA damage, and micronucleus formation. Sustained activation of JNK signaling and modulation of NF-κB pathways were also reported, with partial attenuation by antioxidants, supporting a ROS-mediated mechanism [38]. Ramesh et al. reported that ultrafine magnetite nanoparticles (~9 nm) induced dose-dependent inhibition of proliferation, oxidative stress, antioxidant depletion (GSH and SOD), caspase activation, and apoptosis in rat pulmonary epithelial cells, with pronounced effects at higher concentrations [39]. Similarly, Ahamed et al. demonstrated dose-dependent cytotoxicity, oxidative stress, DNA damage, and apoptosis in human epithelial cell lines (A431 and A549) following exposure to ~25 nm magnetite nanoparticles [40].

Further studies confirmed size-dependent oxidative responses without classical apoptotic activation. Könczöl et al. observed increased superoxide generation, antioxidant imbalance, and p21-mediated cell cycle arrest in A549 and H1299 cells exposed to micro- and nanoscale magnetite particles, in the absence of caspase-3/7 activation [41]. In contrast, oleate-coated magnetite nanoparticles showed high biocompatibility in NIH3T3 fibroblasts, with limited cytotoxicity and vesicular accumulation reported only after prolonged exposure [36]. In hepatocytes, Gokduman et al. demonstrated that magnetite nanoparticle toxicity was dependent on both concentration and exposure pattern, with cumulative dosing resulting in reduced viability, impaired hepatic function, increased ROS generation, and progressive cell death, highlighting the importance of exposure kinetics in toxicity assessment [42]. Wu et al. further showed that ultrasmall Fe_3O_4 nanoparticles (<5 nm) induced enhanced cytotoxicity and hydroxyl radical (·OH) generation, nuclear penetration, and reduced viability in MCF-7 cells, whereas larger particles exhibited lower toxicity [20].

3.2.3. Humans

The presence of magnetite in human tissues was first directly demonstrated by Kirschvink et al., who identified nanometric magnetite crystals in postmortem human brain tissue using SQUID magnetometry and electron microscopy techniques. The morphology and organization of the particles supported an endogenous biomineralization origin [43]. In contrast, Maher et al. identified exogenous iron-rich nanoparticles in cardiac mitochondria of individuals residing in highly polluted urban environments, associated with severe mitochondrial damage and oxidative stress, suggesting a link between inhaled magnetite-rich particulate matter and cardiovascular risk, even at early ages [14].

Table 3. Toxicological effects of magnetite nanoparticles in rat and mouse models.

Author	Biological model	Route of administration	Damage induced / Observed effects
Pauluhn, 2009	*Rattus norvegicus*	Nose-only inhalation	Dose-dependent pulmonary accumulation; reduced pulmonary clearance; lung inflammation (↑ LDH, proteins, PMNs in BAL); cellular infiltration; prolonged particle retention

 doi:10.20944/preprints202601.1266.v1

Pauluhn, 2012	Wistar rat	Nose-only inhalation, subchronic	Pulmonary inflammation; ↑ neutrophils in BAL; histopathological changes in the respiratory tract; ↑ lung and lung-associated lymph node weights; increased septal collagen; NOAEL 4.7 mg/m^3
Szalay et al., 2012	Male Wistar rat	Single intratracheal instillation	Focal pulmonary inflammation; mild pulmonary fibrosis; reduced body-weight gain; decreased relative weights of lung, liver, and kidney
Tada et al., 2012	Fischer 344 rat	Single intratracheal instillation	Increased lung weight; accumulation in alveolar macrophages; inflammatory infiltration; multinucleated cells; pulmonary granulomas; reactive epithelial changes
Jarockyte et al., 2016	Wistar rat	Intramuscular injection	Dose-dependent tissue retention; slow clearance; persistence of nanoparticles at high doses
Matusiak et al., 2017	Male Wistar rat	Intravenous injection	Transient increase in liver mass; elevated hepatic Fe levels; persistent alterations in Ca, Cu, and Zn; no significant changes in body weight
Totsuka et al., 2014	*Mus musculus* (ICR and gpt delta)	Intratracheal instillation (single and repeated)	Pulmonary DNA damage; ↑ oxidative adducts (8-oxodG, HεdG/HεdC); mutagenesis; pulmonary inflammation; granuloma formation
Orel et al., 2015	Male C57BL/6 mouse	Intravenous injection	Mitochondrial alterations in tumor cells; ↑ oxidative stress; ↓ ATP production; inhibition of tumor growth (controlled therapeutic application)
Wu et al., 2022	Male ICR mouse	Intravenous injection	Size-dependent acute and lethal toxicity; cardiotoxicity; ↑ ROS and ·OH; elevated ALT/AST; systemic tissue damage

3.2.4. Mice

In murine models, Totsuka et al. demonstrated that intratracheal instillation of magnetite nanoparticles induced dose-dependent pulmonary DNA damage, oxidative stress markers, inflammation, and increased mutation frequency, supporting a genotoxic mechanism associated with oxidative stress [44]. Conversely, magnetite-based nanocomplexes have been exploited therapeutically. Orel et al. reported enhanced antitumor efficacy of doxorubicin when combined with magnetite nanoparticles and electromagnetic irradiation, highlighting their biomedical potential under controlled conditions [45]. However, Wu et al. showed that intravenous administration of ultrasmall magnetite nanoparticles (<5 nm) induced acute lethality, severe oxidative stress, and cardiac injury at high doses, identifying hydroxyl radical generation as a central mechanism of toxicity [20].

 doi:10.20944/preprints202601.1266.v1

Table 4. In vitro toxicological studies of magnetite (Fe_3O_4) nanoparticles.

Author	Cell model	Exposure type	Induced damage / Observed effects
Könczöl et al., 2011	Human pulmonary epithelial cells (A549)	Direct exposure in culture	Oxidative stress (↑ ROS), mitochondrial membrane potential disruption, DNA damage (Comet assay), micronucleus formation, sustained JNK activation and NF-κB modulation; ROS-dependent genotoxicity
Ramesh et al., 2012	Rat pulmonary epithelial cells (RL-65)	Direct exposure in culture	Dose-dependent inhibition of proliferation, ↑ ROS and lipid peroxidation, ↓ GSH and SOD, activation of caspases-3/-8, DNA fragmentation, and apoptosis
Ahamed et al., 2013	Human epithelial cells A431 (skin) and A549 (lung)	Direct exposure in culture	Dose-dependent cytotoxicity, ↑ LDH, ↑ ROS and MDA, ↓ GSH, DNA damage, and caspase-3/-9-mediated apoptosis
Könczöl et al., 2013	Human cells A549 and H1299	Direct exposure in culture	Size-dependent superoxide radical generation, ↓ GSH, ↑ CAT activity, cell-cycle alteration (↑ sub-G1 population), p21 activation without apoptosis induction
Jarockyte et al., 2016	Mouse embryonic fibroblasts (NIH3T3)	Direct exposure in culture	Perinuclear endocytic internalization, minimal cytotoxicity, mild morphological changes; relatively high biocompatibility
Gokduman et al., 2018	Primary hepatocytes from Lewis rats	Direct exposure in culture (single and cumulative dosing)	Reduced viability, ↑ ROS, impaired hepatic functions (albumin and urea production), time- and accumulation-dependent increase in cell death
Wu et al., 2022	MCF-7 cells (human breast carcinoma)	Direct exposure in culture	Size-dependent toxicity (<5 nm), ·OH generation, ↑ ROS, marked reduction in viability, nuclear entry of ultrasmall nanoparticles, and acute cellular damage

3.2.5. Aquatic and Invertebrate Models

In aquatic models, magnetite nanoparticles impaired sperm motility and induced oxidative stress in rainbow trout spermatozoa [47], while other studies demonstrated either negligible embryotoxicity in *Danio rerio* under low concentrations or pronounced oxidative stress, genotoxicity, and apoptosis depending on exposure route and dose [48]. In invertebrates, reproductive toxicity, neurotoxicity, oxidative stress, and DNA damage were reported in *Caenorhabditis elegans* [50], dipteran insects [51], and mollusks, where magnetite exposure induced lipid peroxidation, protein carbonylation, and genotoxic effects, confirming their sensitivity as biomonitors of nanoparticle exposure [48].

Overall, in vitro studies indicate that magnetite nanoparticles induce cytotoxic and genotoxic effects that are primarily dependent on particle size, dose, and exposure duration rather than on the specific cell type. Dominant toxicity mechanisms consistently involve reactive oxygen species generation, mitochondrial dysfunction, DNA damage, and differential activation of cellular signaling pathways, including JNK, p21, and caspases. Nanoscale and ultrasmall particles (<10–20 nm) exhibit enhanced biological reactivity, increased cellular internalization, and, in some cases, nuclear access, which is associated with elevated oxidative and genotoxic damage. In contrast, micro- and

 doi:10.20944/preprints202601.1266.v1

submicrometric particles predominantly induce cytotoxic effects at higher concentrations. These findings demonstrate that magnetite toxicity is highly dependent on physicochemical properties, emphasizing the importance of particle size, morphology, and aggregation state in risk assessment and in the extrapolation of in vitro outcomes to more complex in vivo models and sensitive biological interfaces.

3.3. Maghemite and Adverse Effects Induced by Exposure in Living Organisms

Toxicological, cytotoxic, and genotoxic evaluations of maghemite (γ-Fe_2O_3) have been conducted predominantly using surface-functionalized or coated nanoparticles, largely motivated by biomedical translation and the pursuit of improved biocompatibility. The evidence across organisms is summarized below, with a more synthetic comparison provided in Tables 5 and 6.

3.3.1. Rats

In Wistar rats, in vivo biocompatibility of ~10 nm spherical γ-Fe_2O_3 nanoparticles functionalized with 3,4-dihydroxyphenethylamine (fluorescent labeling; no protective biocompatible shell) was assessed after a single intravenous dose (0.8 mg/kg). Rapid systemic clearance was reported (≈40% removed from circulation at 24 h; ≈75% at 72 h), mainly via urinary excretion; however, leukocytosis (~50% increase) and inflammatory infiltration in lung, liver, and kidney were detected histologically. These findings indicate that fast clearance does not preclude peripheral inflammatory injury, supporting the need for coating/targeting strategies and exposure-time control prior to clinical consideration [52].

3.3.2. Cell models

In human dermal fibroblasts, DMSA-coated γ-Fe_2O_3 nanoparticles (~6 nm) were tested across 10^{-6}–10^{-1} g/L and 2–48 h. Only a mild viability decrease was observed at lower concentrations (10^{-6}–10^{-3} g/L) in early exposures, while no genotoxicity was detected by the Comet assay. Increased mitochondrial activity at higher concentrations was attributed to reduced effective cell–particle interaction due to aggregation, consistent with a protective role of DMSA in limiting direct contact with the oxidizing core; longer-term and cross-model validation was nevertheless recommended [16].In murine NIH/3T3 fibroblasts, sub-10 nm γ-Fe_2O_3 formulations showed near-complete viability after 24 h (typically 1–10 mM), whereas cellular uptake depended strongly on coating-driven colloidal stability: citrate-coated particles destabilized in serum-containing medium, formed aggregates, sedimented, and yielded high apparent uptake (~250 pg Fe/cell), whereas PAA2K-coated particles remained colloidally stable and showed markedly lower uptake (<30 pg/cell). Thus, coating and dispersion stability were identified as primary determinants of uptake and biocompatibility profiles [53].

In human endothelial cells (HUVEC; Ea.hy 926), ~10 nm γ-Fe_2O_3 nanoparticles functionalized with 3,4-dihydroxyphenethylamine were efficiently internalized and localized to cytoplasm and membrane-bound organelles without nuclear entry. Reduced viability at 48–72 h, increased cytotoxicity from 24 h, and elevated ROS were reported, whereas caspase-3 activation was not detected, supporting a predominantly non-apoptotic (necrosis-like) mechanism under the tested conditions and with limited dose dependence [52].In bovine spermatozoa, DMSA-coated γ-Fe_2O_3 nanoparticles (5.3–8.1 nm) tested for 4 h (0.015–0.06 mg Fe/mL) did not affect motility, membrane integrity, acrosomal reaction, or ultrastructure. Electron microscopy revealed agglomerates near the sperm head without evidence of cytoplasmic internalization, supporting low acute toxicity in this model while motivating broader safety confirmation [54].

3.3.3. Humans

Postmortem human brain tissue analyses provided direct evidence of iron-oxide nanoparticles, with crystallographic data indicating a substantial fraction consistent with maghemite, especially

 doi:10.20944/preprints202601.1266.v1

among smaller particles (predominantly 10–70 nm) frequently organized in clusters of ~50–100 particles. The absence of geological contaminants and morphological similarities to biogenic iron oxides supported an in situ, biological origin [43]. In cardiac tissue from young individuals chronically exposed to severe urban air pollution, exogenous iron-rich nanoparticles—mainly magnetite and maghemite (15–40 nm, rounded)—were identified inside myocardial mitochondria, accompanied by marked mitochondrial structural disruption and increased oxidative/ER stress markers. Translocation of inhaled Fe-rich nanoparticles to the heart was proposed as a plausible mechanism contributing to early-life mitochondrial dysfunction and potential cardiovascular risk [14].

3.3.4. Mice

In BALB/cJ mice, polyacrylic-acid–coated γ-Fe_2O_3 nanoparticles (~6.8 nm) administered intravenously (10 mg/kg; 100 µL) accumulated rapidly in liver (within 1 h), followed by kidney and spleen, remaining detectable up to 96 h. Renal function (glomerular filtration and acid–base balance) was not altered, whereas a transient reduction in mean arterial pressure (12–24 h) and reversible mesenteric artery contractility changes were observed, indicating mild, acute, reversible cardiovascular effects without renal injury [55].In pregnant ICR mice, oral exposure to spherical γ-Fe_2O_3 nanoparticles (20–30 nm) during early gestation (1–100 mg/kg/day for 7 days; evaluation day 15) produced dose-dependent developmental toxicity at the highest dose, including increased fetal resorption/embryonic death and reduced placental weight. Placental histology showed structural disruption, alongside reduced Crat expression, decreased mitochondrial ATP synthesis, and oxidative stress alterations, implicating mitochondrial dysfunction and oxidative stress as central drivers at elevated exposure [47].

3.3.5. Fish

In *Poecilia reticulata*, chronic aqueous exposure (21 days) to environmentally relevant citrate-functionalized γ-Fe_2O_3 nanoparticles (~3.97 ± 0.85 nm; 0.3 mg Fe L^{-1}; n≈200) induced progressive DNA damage and time-dependent increases in erythrocytic nuclear abnormalities (e.g., micronuclei and other nuclear morphologies), demonstrating significant genotoxic and mutagenic effects under low but sustained exposure [57]. Complementary work reported enlarged and denser melanomacrophage centers (MMC) and hepatic immune activation (MMC aggregates, steatosis, exudates, hemorrhagic foci), supporting MMCs as sensitive biomarkers for nanoparticle-associated hepatic toxicity and reinforcing *P. reticulata* as a responsive bioindicator for iron-oxide nanomaterials [58].

In zebrafish embryos, developmental effects were reported following aqueous exposure, including delayed hatching without major mortality in one study [58], whereas another study documented substantial developmental toxicity (≈30% mortality at 100 µg/L by 120 hpf), reduced hatching, impaired growth and heart rate, behavioral alterations, early apoptosis, mitochondrial dysfunction (ΔΨm loss, ATP reduction), and oxidative stress (↑MDA; ↓CAT/SOD), supporting a mechanistic axis of mitochondrial impairment plus oxidative stress [47].

In rainbow trout (*Oncorhynchus mykiss*), exposure to γ-Fe_2O_3 (1–25 mg/L, 10 days) induced severe histopathological damage in kidney, liver, and gills, together with iron accumulation (notably in liver) and oxidative stress responses, confirming ecotoxicological potential under higher aqueous concentrations [59]. In male *P. reticulata*, chronic exposure (0.3–3.0 µg L^{-1}; 14–21 days) did not alter sexual behavior but induced testicular histopathology and spermatogenesis disruption, indicating potential reproductive impairment under sustained exposure [60]. Conversely, in *Oreochromis niloticus*, acute exposure (24–96 h; 0–100 mg/L) produced transient bioaccumulation (blood, gills, hepatopancreas, muscle; digestive tract) without relevant genotoxicity (micronucleus/Comet) or major histological alterations, and tissue iron declined during recovery, indicating low acute toxicity with reversible accumulation under the evaluated conditions [49].

 doi:10.20944/preprints202601.1266.v1

3.3.6. Primates

In non-human primates (Cebus spp.), intravenous administration of DMSA-coated γ-Fe_2O_3 nanoparticles (~8 nm; 0.5 mg Fe/kg) produced preferential distribution to lungs, liver, and kidneys, with progressive reduction of agglomerates by 30–90 days. Particles were detected mainly in alveolar macrophages, hepatocytes, and renal proximal tubules, while severe lesions, necrosis, and hemorrhage were not observed; only mild long-term hepatic alterations were reported. Hematological, biochemical, behavioral, and body-weight parameters remained within physiological ranges, supporting overall biocompatibility and progressive clearance in this primate model [61].

3.3.7. Mollusks

In *Mytilus galloprovincialis*, exposure to γ-Fe_2O_3 nanoparticles (or zeolite-incorporated formulations) produced measurable oxidative stress and cellular damage endpoints, including increased ROS, TBARS, protein carbonylation, DNA damage, ubiquitin conjugates, and shifts in pro-/antioxidant balance (PAB). Stronger responses were reported for zeolite-incorporated nanoparticles under the tested conditions, indicating formulation-dependent toxicity in marine invertebrate systems. Overall, the available evidence indicates that maghemite (γ-Fe_2O_3) nanoparticles exhibit a toxicity profile that is strongly modulated by surface functionalization, particle size, and exposure route, resulting in outcomes that range from high biocompatibility to organ-specific inflammatory, oxidative, and developmental effects. These findings highlight the dual nature of maghemite as both a promising nanomaterial for biomedical applications and a potential environmental contaminant, underscoring the need for integrated risk assessments that consider realistic exposure scenarios, biodistribution kinetics, and oxidative stress–mediated mechanisms.

Table 5. Biological effects of maghemite (γ-Fe_2O_3) nanoparticles in mammalian models.

Author	Biological model	Route of administration	Induced damage / Observed effects
Hanini et al., 2011	Wistar rats	Single intravenous injection	~50% increase in leukocyte count; inflammatory infiltration and cellular damage in lung, liver, and kidney; no changes in body weight or severe clinical signs
Iversen et al., 2013	BALB/cJ mice	Intravenous injection	Significant but transient decrease in mean arterial pressure (12–24 h) and reversible reduction in arterial contractility; no renal damage
Huang et al., 2019	Pregnant ICR female mice	Oral (gastrointestinal) exposure	At high doses: fetal resorption and embryonic death, reduced placental weight, placental histological alterations, decreased *Crat* expression, reduced mitochondrial ATP production, and oxidative stress–related alterations
Monge-Fuentes et al., 2011	Primate (*Cebus* spp.)	Intravenous injection	Mild long-term hepatic alterations; particle presence in alveolar macrophages, hepatocytes, and renal tubules; no necrosis, hemorrhage, or hematological or behavioral alterations

 doi:10.20944/preprints202601.1266.v1

Table 5 summarizes in vivo studies assessing the biological effects of maghemite (γ-Fe_2O_3) nanoparticles in mammalian models, considering exposure route and associated outcomes. In Wistar rats, single intravenous administration induced a subclinical systemic inflammatory response, evidenced by leukocytosis and inflammatory infiltration in peripheral organs without severe clinical manifestations. In BALB/cJ mice, intravenous exposure resulted in acute, mild, and reversible cardiovascular effects, with no structural renal damage. By contrast, oral exposure during gestation in ICR females revealed a pronounced embryotoxic potential at high doses, characterized by placental alterations, oxidative stress, and mitochondrial metabolic impairment. In non-human primates (Cebus spp.), preferential biodistribution to lungs, liver, and kidneys was observed, with only mild long-term hepatic changes and no severe structural lesions, indicating relative biocompatibility in this model.

Overall, in vitro evidence indicates that the biocompatibility of maghemite nanoparticles is strongly dependent on cell type, surface coating, and colloidal stability. Minimal or no effects are generally reported in fibroblasts and spermatozoa when DMSA-coated formulations are used, whereas in human endothelial cells, cytotoxicity associated with increased reactive oxygen species and non-apoptotic cell death mechanisms has been observed. These findings underscore the necessity of assessing multiple cellular models and physicochemical parameters before extrapolating the safety of maghemite nanoparticles to in vivo systems.

Table 6. In vitro studies on cytotoxicity and biocompatibility of maghemite (γ-Fe_2O_3) nanoparticles in cellular models.

Author	Biological model (cells)	Exposure type	Induced damage / Observed effects
Auffan et al.	Human dermal fibroblasts	In vitro exposure	Mild reduction in cell viability at 10^{-6}–10^{-3} g/L (2–24 h); absence of genotoxicity (Comet assay); increased mitochondrial activity at higher concentrations; no detectable genetic damage
Safi et al.	Murine fibroblasts (NIH/3T3)	In vitro exposure	No cytotoxic effects observed (≈100% viability); cellular uptake dependent on surface coating: high uptake with citrate (~250 pg Fe/cell) and low uptake with PAA2K (<30 pg/cell); no associated cellular damage
Hanini et al.	Human endothelial cells (HUVEC, Ea.hy 926)	In vitro exposure	Significant reduction in viability at 48–72 h; increased cytotoxicity from 24 h; elevated ROS production; absence of caspase-3 activation, suggesting predominantly necrotic cell death
Caldeira et al.	Bovine spermatozoa	In vitro exposure	No alterations in motility, membrane integrity, acrosomal reaction, or ultrastructure; presence of extracellular aggregates without internalization; absence of toxic effects

 doi:10.20944/preprints202601.1266.v1

3.4. Hematite and Its Biological Effects Following Exposure

This section synthesizes studies evaluating the biological effects of hematite exposure across multiple experimental models, based on the available literature to date. A concise overview of these findings is provided in Table 5.

3.4.1. Rats

Early in vivo evidence was provided by Garry et al., who evaluated the genotoxic effects of hematite (Fe_2O_3) administered alone or combined with benzo[a]pyrene (B[a]P) in adult male Sprague–Dawley rats via endotracheal instillation (3.75 mg/kg). While hematite alone did not induce detectable DNA damage, B[a]P—particularly when adsorbed onto hematite particles—produced significant genotoxic effects in pulmonary cells, lymphocytes, and hepatocytes, indicating that hematite can act as a carrier that enhances PAH genotoxicity [62].

Subsequent studies in Wistar rats demonstrated that repeated intravenous exposure to hematite nanoparticles (30–35 nm) induced dose- and time-dependent hematological alterations and systemic oxidative stress, including leukocytosis, lipid peroxidation, and reduced antioxidant defenses, without detectable DNA damage in blood cells [63]. Intranasal exposure studies further revealed organ-specific proteomic alterations in brain, liver, and lung, highlighting oxidative, inflammatory, and neurochemical pathway disruptions that are not captured by conventional toxicological endpoints [64]. In contrast, orally administered green-synthesized hematite nanoparticles produced no systemic toxicity at low doses (≤10 mg/kg), although histopathological alterations were observed at higher doses, underscoring the relevance of dose and synthesis route [65].

3.4.2. Cells

In vitro studies consistently indicate low intrinsic cytotoxicity of hematite particles, with biological responses strongly modulated by particle size, surface properties, and co-exposures. Early work using alveolar macrophages demonstrated efficient phagocytosis of respirable hematite with minimal cytotoxicity, except at high particle burdens [66]. Similarly, hematite alone did not induce genotoxicity in isolated rat cells, whereas B[a]P adsorbed onto hematite significantly amplified DNA damage, confirming the role of surface adsorption in toxicity enhancement [15].

Comparative studies using human pulmonary cell lines showed that nanometric hematite exhibits greater cytotoxic and oxidative potential than micrometric particles at high concentrations, although aggregation and protein corona formation strongly modulated these effects [67]. Other investigations reported minimal acute toxicity across epithelial and macrophage models [68], while intestinal and placental barrier models revealed size-dependent disruption of epithelial integrity without overt cell death, highlighting sublethal but functionally relevant effects [69,70]. Additional studies demonstrated that morphology, crystallinity, and surface defects critically influence cellular uptake and ROS generation [71], whereas most cellular systems tolerated hematite exposure at moderate concentrations [58,72,74,75].

3.4.3. Amphibians

Embryotoxicity assessments using *Xenopus laevis* (FETAX protocol) indicated low acute toxicity of hematite nanoparticles, with developmental effects observed only at very high concentrations, suggesting limited short-term hazard under realistic exposure scenarios [73].

3.4.4. Humans

Human data remain scarce. Occupational exposure studies reported pulmonary fibrosis and iron deposition following chronic inhalation of respirable hematite dust in mining settings [76]. However, large retrospective cohort analyses of hematite miners did not demonstrate increased lung cancer mortality under controlled industrial conditions, emphasizing the importance of co-exposures and workplace controls [77].

 doi:10.20944/preprints202601.1266.v1

3.4.5. Mice

Murine models demonstrated that intranasally administered hematite particles can access the central nervous system via olfactory and trigeminal pathways, resulting in iron accumulation and neuronal damage in specific brain regions [78]. In contrast, stereotactic hippocampal administration of nanorhombohedral hematite showed efficient microglial uptake without inflammatory activation, supporting context-dependent neurocompatibility [72]. Oral exposure to biosynthesized hematite nanoparticles did not induce acute systemic toxicity [79].

3.4.6. Fish

In aquatic models, hematite nanoparticles generally exhibited low developmental toxicity in zebrafish embryos [47], whereas rainbow trout exposed to higher concentrations showed dose-dependent histopathological alterations and oxidative stress responses, indicating sublethal toxicity under elevated exposure conditions [59].

3.4.7. Guinea Pigs

Classic inhalation and instillation studies in guinea pigs demonstrated mild to moderate pulmonary inflammation and persistent biochemical and mitochondrial alterations in lung tissue, even in the absence of overt fibrosis, highlighting long-term metabolic consequences of inhaled hematite dust [80–82].

3.4.8. Crustaceans

Finally, biosynthesized hematite nanoparticles showed low acute toxicity in *Artemia salina*, with mild oxidative and neurochemical responses at high concentrations, suggesting limited short-term ecotoxicological risk under environmentally relevant conditions [79].

Table 7 summarizes key studies employing animal models to assess the toxicological effects of hematite (Fe_2O_3) particles and nanoparticles under different exposure routes. The evidence spans early guinea pig inhalation studies of respirable dust to more recent rat and mouse models addressing biodistribution, systemic toxicity, neurological effects, hematological alterations, and organ-specific molecular responses. Overall, hematite toxicity was shown to be strongly dependent on exposure route, particle size, and exposure context, ranging from persistent inflammatory and metabolic alterations to low acute toxicity under specific conditions. Several studies further highlight systemic iron mobilization and its interaction with mitochondrial, genotoxic, and neurotoxic processes, underscoring the importance of considering both isolated and co-exposure scenarios in biological risk assessment of iron oxides.

Table 7. Biological effects of hematite (Fe_2O_3) exposure in animal models according to the route of administration.

Author (year)	Biological model	Route of administration	Induced damage / Observed effects
Carleton (1927)	Guinea pig (*Cavia porcellus*)	Inhalation of fine dust in a closed chamber	Mild–moderate pulmonary inflammatory response (alveolar epithelial proliferation, transient bronchitis); dust migration to subpleural regions and lymph nodes; progressive pulmonary clearance without fibrosis; limited systemic iron accumulation, mainly in spleen
Jaiswal et al. (1979)	Guinea pig (*Cavia porcellus*)	Intratracheal instillation	Persistent pulmonary metabolic alterations: increased fructose-1,6-bisphosphatase, decreased G6PD, marked reduction of mitochondrial succinate dehydrogenase and carbonic anhydrase; mitochondrial dysfunction without overt fibrosis

 doi:10.20944/preprints202601.1266.v1

Das et al. (1983)	Guinea pig (*Cavia porcellus*)	Intratracheal instillation	Systemic iron mobilization to liver, spleen, bone marrow, kidney, and heart; pulmonary mitochondrial accumulation; increased cytochrome c oxidase and altered mitochondrial permeability, without marked pulmonary fibrosis
Wang et al. (2007)	Male CD-ICR mouse	Intranasal instillation	Brain iron accumulation in olfactory bulb and brainstem; increased Fe(III); neuronal degeneration in hippocampal CA3; evidence supporting transport via olfactory and trigeminal pathways
Lewis et al. (2016)	MacGreen transgenic mouse	Bilateral stereotactic injection into dorsal hippocampus	Uptake by hippocampal microglia without inflammatory activation or apparent structural alterations at 24 h
Rajendran et al. (2021)	Swiss albino mouse (*Mus musculus*)	Oral gavage administration	No mortality or acute toxicity; hematological, biochemical, and histopathological parameters largely normal, with a slight increase in bilirubin
Garry et al. (2003)	Male Sprague–Dawley rat	Endotracheal instillation	Hematite alone showed no genotoxicity; B[a]P and B[a]P-coated hematite induced significant DNA damage, indicating enhancement under co-exposure
Gaharwar & Paulraj (2015)	Male Wistar rat	Intravenous injection	Dose- and time-dependent hematological and inflammatory alterations; systemic oxidative stress without detectable genotoxic damage

Table 8 compiles major in vitro studies using cellular models to evaluate the biological effects of hematite (Fe_2O_3) particles and nanoparticles across respiratory, intestinal, placental, renal, and neural systems. Overall, hematite exhibited low baseline cytotoxicity in multiple cell types under acute exposure conditions; however, responses were strongly dependent on particle size, concentration, exposure duration, and physicochemical properties. Notably, smaller nanoparticles and particles with specific surface characteristics showed enhanced cellular internalization, increased reactive oxygen species generation, disruption of epithelial barrier integrity, and mitochondrial dysfunction, even in the absence of immediate cell death. Additionally, several studies demonstrated that hematite can potentiate the genotoxicity of co-occurring contaminants when acting as a particulate carrier, emphasizing the relevance of physicochemical interactions and co-exposure scenarios in iron oxide toxicological assessments.

Table 8. In vitro studies in cellular models exposed to hematite (Fe_2O_3) particles and nanoparticles.

Author (year)	Biological model	Exposure type	Induced damage / Observed effects
Warshawsky et al. (1994)	Alveolar macrophages	Direct in vitro exposure	Efficient particle phagocytosis; preserved viability at most concentrations; moderate viability reduction (~67%) only at the highest dose
Garry et al. (2004)	Alveolar macrophages, pulmonary cells, hepatocytes, and peripheral lymphocytes from Sprague–Dawley rats	In vitro exposure	Hematite alone: no genotoxicity; B[a]P alone: DNA damage; B[a]P adsorbed onto Fe_2O_3: marked enhancement of genotoxic damage in a cell-type–dependent manner, demonstrating a vector effect of hematite

 doi:10.20944/preprints202601.1266.v1

Bhattacharya et al. (2012)	Human lung cells (BEAS-2B and IMR-90)	In vitro exposure	Intracellular internalization; reduced viability and increased ROS at ≥50 μg/mL, more pronounced for nanoparticles; toxicity strongly modulated by agglomeration and biomolecule interactions
Freyria et al. (2012)	Murine alveolar macrophages (MH-S) and human pulmonary epithelial cells (A549)	In vitro exposure	No cytotoxicity, apoptosis/necrosis, DNA damage, or nitric oxide production; low acute toxicity under the evaluated conditions
Kalive et al. (2012)	Human intestinal epithelial cells (Caco-2)	Single exposure	Size-dependent disruption of epithelial barrier integrity; 17 nm particles reduced TEER, altered cell junctions and epithelial architecture without inducing early cell death
Faust et al. (2014)	Human placental epithelial cells (BeWo b30)	In vitro exposure	Progressive and irreversible TEER reduction with 50 and 78 nm particles; increased ROS, tight junction disruption, and apoptotic-related alterations
Cardillo et al. (2016)	Canine renal epithelial cells (MDCK)	In vitro exposure	Morphology-dependent internalization; elongated particles showed higher uptake; significant ROS increase observed only for particles with specific surface characteristics
Lewis et al. (2016)	Primary microglia from MacGreen mice and N9 microglial cell line	In vitro exposure	Size-dependent internalization; overall low cytotoxicity, with significant effects only at the highest concentration and longer exposure times
Lee et al. (2020)	Human HeLa cells	In vitro exposure	Minimal effects at ≤50 μg/mL; reduced viability, oxidative stress, and cell death observed at 100 μg/mL

4. Discussion

Studies addressing the biological effects induced by exposure to iron oxide particles consistently demonstrate that toxicological outcomes are critically governed by physicochemical and experimental parameters, including particle size and shape, surface coating, applied concentration, exposure duration, and route of administration. Collectively, these variables determine the magnitude of observed damage, biocompatibility, cellular internalization efficiency, and the molecular mechanisms activated across biological models.

4.1. Cellular Models

Magnetite has been the most extensively evaluated iron oxide in vitro, using human and rodent cell lines such as pulmonary epithelial cells (A549, H1299), tumor cells (A431, MCF-7), murine fibroblasts (NIH/3T3), and primary rat hepatocytes. Across these models, reduced cell viability, oxidative stress, mitochondrial dysfunction, DNA damage, micronucleus formation, and activation of signaling pathways (JNK, TNFR, p21) and caspase-mediated apoptosis (caspases-3, -7, -8, and -9) have been consistently reported [20,36,38–42]. A strong size dependency was observed, with nanoparticles <10 nm exhibiting markedly higher toxicity, particularly under oxidative conditions such as hydrogen peroxide co-exposure [20]. Higher concentrations and prolonged exposures further exacerbated these effects, including cell-cycle alterations and depletion of antioxidant defenses such as GSH [39,40]. Surface coatings were shown to play a dual role, either attenuating toxicity by limiting direct cell–particle interactions [36] or enhancing cellular damage when coatings such as citrate promoted uptake and reactivity [20].

 doi:10.20944/preprints202601.1266.v1

Hematite has been investigated across a broader spectrum of cellular systems, including macrophages, lymphocytes, pulmonary, intestinal, placental, renal, embryonic, and neural cells. Reported effects ranged from efficient phagocytosis and intracellular accumulation to epithelial barrier disruption, oxidative stress, mitochondrial impairment, apoptosis, and gene expression changes [15,47,58,66–75]. Under acute exposure conditions (≤24 h) and low-to-moderate concentrations, particularly in resilient cells such as alveolar macrophages, hematite generally exhibited low cytotoxicity [66,68]. In contrast, higher concentrations (≥50 μg/mL) and longer exposures resulted in increased ROS production, mitochondrial damage, and reduced viability [58,75]. Importantly, hematite acted as an effective particulate carrier for benzo[a]pyrene, significantly amplifying genotoxic and cytotoxic responses through adsorption-mediated co-exposure [15].

Compared with magnetite and hematite, maghemite has been evaluated in fewer cellular models, mainly human dermal fibroblasts, murine fibroblasts (NIH/3T3), human endothelial cells (HUVEC), and bovine spermatozoa. Observed effects generally included mild reductions in viability, cellular uptake, oxidative stress, ROS generation, and necrotic cell death, with overall lower toxicity profiles [16,52–54]. These findings may partly reflect the more limited experimental coverage. Nevertheless, surface functionalization emerged as a key determinant, with some coatings reducing toxicity by stabilizing particles, while others enhanced uptake and damage [53]. Overall, in vitro evidence indicates that magnetite exhibits the highest cytotoxic potential among iron oxides, followed by hematite, whereas maghemite appears comparatively less harmful. However, these trends are strongly modulated by surface chemistry, particle size, morphology, and concentration, underscoring the need for standardized experimental frameworks and deeper mechanistic investigations to improve cellular-level risk assessment.

4.2. Rat Models

Rattus norvegicus has been widely employed to investigate iron oxide toxicity, enabling evaluation of organ accumulation, inflammatory responses, genotoxicity, and systemic effects under controlled variations of size, coating, exposure route, dose, and duration. Across studies, magnetite consistently induced the most severe effects, particularly following inhalation and intratracheal exposure. Subchronic inhalation resulted in persistent pulmonary accumulation, bronchiolar hyperplasia, inflammatory cell infiltration, enzymatic release (LDH, NAG), and structural lung damage at moderate concentrations (≥3 mg/m^3) [33,34]. These findings were corroborated by reports of pulmonary granulomas, epithelial remodeling, mild fibrosis, weight loss, hepatorenal involvement, and prolonged particle retention, indicating slow clearance and systemic distribution [18,35,36]. Maghemite exposure has been primarily investigated due to its biomedical relevance. In contrast to magnetite, oral administration emerged as the most deleterious route, despite the larger particle size (PM1.0 range), likely due to higher applied doses. Severe outcomes included fetal resorption, embryonic lethality, placental structural damage, and compromised mitochondrial energy metabolism during development [47,55].

Hematite exhibited an intermediate and highly context-dependent toxicity profile. Endotracheal administration of respirable particles did not induce intrinsic genotoxicity, but markedly enhanced benzo[a]pyrene toxicity through adsorption mechanisms [62]. Intravenous exposure mainly triggered oxidative stress and immunohematological alterations without DNA damage [63], whereas intranasal exposure produced the most pronounced effects, including neurotoxicity, inflammation, oxidative stress, neurotransmitter disruption, and organ-specific proteomic alterations [64]. Collectively, these findings indicate that although all iron oxides can induce adverse effects in rats, magnetite is consistently the most toxic, particularly via inhalation and intratracheal routes. Maghemite shows route-specific toxicity dominated by oral exposure, while hematite responses are more dependent on experimental context, with intranasal exposure posing the greatest risk due to neurotoxic outcomes.

 doi:10.20944/preprints202601.1266.v1

4.3. Mouse Models

Consistent with rat studies, mouse models (Mus musculus) identified magnetite as the most toxic iron oxide, with severity strongly influenced by particle size, coating, dose, and exposure route. Toxicity increased with decreasing particle size and absence of surface coatings, with intravenous exposure producing the most severe systemic effects and intranasal exposure associated with genotoxicity and neurotoxicity [20,44,45]. Maghemite studies in mice revealed more pronounced systemic and developmental toxicity, likely reflecting specific experimental designs. Intravenous exposure resulted in organ accumulation, transient hypotension, and vascular effects [55], while oral exposure was associated with fetal resorption, embryonic death, and placental histopathology, contrasting sharply with magnetite outcomes. For hematite, intranasal exposure again emerged as the most hazardous route, inducing neurotoxic effects and neuronal morphological alterations. In contrast, direct stereotactic injection into the brain did not elicit damage, likely due to differences in particle size (PM1.0 vs. PM2.5) and exposure context [72,78]. Overall, magnetite remains the most toxic iron oxide in murine systems, particularly in the ultrafine fraction and without surface coatings.

4.4. Human Evidence

Human data remain limited and methodologically constrained. Nevertheless, available evidence indicates marked differences among iron oxides. Magnetite is the only oxide with documented chronic environmental inhalation data, showing translocation to cardiac tissue and mitochondria, accompanied by severe structural damage, albeit in very small sample sizes [14]. Direct toxicity of maghemite in humans has not yet been clearly established, as available studies did not isolate this phase independently [43]. Hematite has been evaluated primarily in occupational contexts, where chronic exposure produced progressive inflammatory responses without definitive conclusions regarding carcinogenic risk [76,77]. Taken together, existing human evidence supports magnetite as the most biologically aggressive iron oxide, while emphasizing the need for more controlled and systematic investigations.

4.5. Knowledge Gaps and Current Limitations

Despite substantial experimental evidence on the biological activity of iron oxide particles, several critical knowledge gaps and methodological limitations persist. First, many experimental particles lack representativeness of real atmospheric particulate matter. Commercially synthesized or surface-engineered nanoparticles often differ from environmental particles in aggregation state, surface chemistry, and coexistence with other contaminants, limiting direct extrapolation to real-world air pollution scenarios. Second, particle size classification remains insufficiently standardized. While PM2.5 and PM10 are commonly reported, the PM1.0 fraction—characterized by higher reactivity, deeper tissue penetration, and greater toxicological relevance—remains underexplored, despite its increasing prevalence in urban and traffic-related environments.

Third, contradictory findings regarding magnetite toxicity, surface coating effects, and apparent biocompatibility of some formulations highlight the complex, non-linear interactions among size, aggregation, dose, exposure duration, and biological context. Fourth, most studies rely on acute or short-term exposures at relatively high concentrations, whereas data on chronic low-dose exposure—more representative of environmental and occupational conditions—remain scarce, particularly for inhalation scenarios where cumulative effects are likely underestimated.

Finally, insufficient integration exists between atmospheric sciences and experimental toxicology. Few studies directly link detailed physicochemical and magnetic characterization of iron-rich particles with biological responses within unified experimental frameworks, limiting translation to risk assessment and air-quality management. Overall, these gaps underscore the need for multidisciplinary approaches that integrate realistic atmospheric particle characterization with biologically relevant models, promote experimental standardization, and prioritize environmentally relevant exposure scenarios to improve assessment of iron oxide-associated health risks.

 doi:10.20944/preprints202601.1266.v1

5. Conclusions

The body of evidence synthesized in this review demonstrates that iron oxide particles constitute a biologically active and mechanistically complex class of environmental contaminants whose toxicological behavior cannot be generalized across crystalline phase, particle size, or exposure scenario. Instead, adverse outcomes emerge from the dynamic interplay between physicochemical properties—particularly particle size, surface chemistry, aggregation state, and magnetic characteristics—and biological context, including exposure route, dose, duration, and organismal susceptibility.

Across experimental systems, magnetite (Fe_3O_4) consistently exhibits the highest toxic potential, especially within the ultrafine and nanoscale fractions. Its strong redox activity, mixed-valence structure, and high cellular internalization capacity underpin pronounced oxidative stress, mitochondrial dysfunction, genotoxicity, inflammatory activation, and, under certain conditions, acute systemic toxicity. These effects are most evident following inhalation or intratracheal exposure, routes that closely resemble environmentally relevant air pollution scenarios. Importantly, human and animal evidence converges in identifying magnetite-rich particulate matter as capable of translocating beyond the respiratory tract, reaching cardiovascular and neural tissues, where it may compromise mitochondrial integrity and cellular homeostasis.

Hematite (α-Fe_2O_3) displays a more context-dependent toxicity profile. While often characterized by low intrinsic cytotoxicity under acute exposure conditions, hematite exerts biologically relevant effects through indirect mechanisms, particularly its role as a particulate carrier that enhances the genotoxicity and cellular uptake of co-existing contaminants such as polycyclic aromatic hydrocarbons. Additionally, nanoscale hematite particles can disrupt epithelial barriers, alter mitochondrial function, and induce neurotoxic effects when exposure occurs via intranasal routes, underscoring the importance of exposure pathway and particle size in risk evaluation.

Maghemite (γ-Fe_2O_3) generally exhibits the lowest apparent toxicity among the iron oxides reviewed, particularly when stabilized with biocompatible surface coatings. However, this relative biocompatibility is not universal. Developmental toxicity, reproductive effects, vascular alterations, and oxidative stress responses have been reported under high-dose, chronic, or gestational exposure scenarios, indicating that maghemite cannot be regarded as inherently benign. Surface functionalization, colloidal stability, and exposure timing emerge as decisive modulators of its biological impact.

Collectively, the reviewed evidence reveals that oxidative stress and mitochondrial dysfunction represent central and unifying mechanisms across iron oxide types, with downstream activation of inflammatory signaling, barrier disruption, and genotoxic pathways. Crucially, toxicity thresholds and outcomes differ markedly between acute high-dose experimental designs and the chronic low-dose exposures characteristic of real-world environmental and occupational settings—conditions that remain insufficiently explored.

From an environmental health perspective, this review highlights a critical disconnect between atmospheric science and toxicology. Many experimental studies rely on synthetic or highly controlled nanoparticles that do not adequately represent the physicochemical complexity of iron-rich particulate matter present in urban air pollution. Integrating magnetic, mineralogical, and chemical characterization of real airborne particles with biologically relevant exposure models is therefore essential to improve hazard identification and risk assessment.

In this context, magnetic biomonitoring emerges as a powerful and underutilized tool for bridging this gap. By enabling the detection, source attribution, and spatial mapping of iron oxide–rich particulate matter in complex environments, magnetic approaches provide a direct link between particle composition and potential biological relevance. When coupled with toxicological evidence, such techniques can significantly enhance exposure assessment frameworks, particularly in urban settings where traffic-related emissions dominate.

In conclusion, iron oxide particles—especially magnetite-rich fractions—should be recognized as active contributors to particulate matter–associated health risks rather than inert components of

 doi:10.20944/preprints202601.1266.v1

airborne dust. Advancing the field will require standardized particle characterization, environmentally realistic exposure scenarios, and multidisciplinary approaches that integrate atmospheric monitoring with mechanistic toxicology. Such efforts are essential to refine regulatory strategies, protect vulnerable populations, and better understand the role of iron-rich particles in air pollution–related disease.

Supplementary Materials: The following supporting information can be downloaded at the website of this paper posted on Preprints.org.

Data availability: Data sharing is not applicable to this article, as no new data were generated. The reviewed articles are publicly available online.

Acknowledgments: The authors wish to thank the support of the project "CBF-2025-I-4343 (Basic and Frontier Science Call) and the Mexican National Council for Humanities, Science, and Technology (CONAHCYT) for the scholarship granted to MSc Oscar Rodolfo Hernandez Montoya to pursue doctoral studies and conduct this research. We also thank the anonymous reviewers for their insightful comments and suggestions, which greatly improved this manuscript.

Conflicts of Interest: The authors declare no conflict of interest.

References

1. Campos, E.A.; Pinto, D.V.B.S.; Oliveira, J.I.S.D.; Mattos, E.D.C.; Dutra, R.D.C.L. Synthesis, characterization and applications of iron oxide nanoparticles: A short review. J. Aerosp. Technol. Manag. 2015, 7, 267–276.
2. Benhammada, A.; Trache, D.; Kesraoui, M.; Tarchoun, A.F.; Chelouche, S.; Mezroua, A. Synthesis and characterization of α-Fe_2O_3 nanoparticles from different precursors and their catalytic effect on the thermal decomposition of nitrocellulose. Thermochim. Acta 2020, 686, 178570.
3. Cornell, R.M.; Schwertmann, U. The Iron Oxides: Structure, Properties, Reactions, Occurrences and Uses; Wiley-VCH: Weinheim, Germany, 2003.
4. Teja, A.S.; Koh, P.Y. Synthesis, properties, and applications of magnetic iron oxide nanoparticles. Prog. Cryst. Growth Charact. Mater. 2009, 55, 22–45.
5. Laurent, S.; Forge, D.; Port, M.; Roch, A.; Robic, C.; Vander Elst, L.; Muller, R.N. Magnetic iron oxide nanoparticles: Synthesis, stabilization, vectorization, physicochemical characterizations, and biological applications. Chem. Rev. 2008, 108, 2064–2110.
6. Dadfar, S.M.; Roemhild, K.; Drude, N.I.; von Stillfried, S.; Knüchel, R.; Kiessling, F.; Lammers, T. Iron oxide nanoparticles: Diagnostic, therapeutic and theranostic applications. Adv. Drug Deliv. Rev. 2019, 138, 302–325.
7. Ogbezode, J.E.; Ezealigo, U.S.; Bello, A.; Anye, V.C.; Onwualu, A.P. A narrative review of the synthesis, characterization, and applications of iron oxide nanoparticles. Discover Nano 2023, 18, 125.
8. Wang, F.; Zhou, L.; Mu, D.; Zhang, H.; Zhang, G.; Huang, X.; Xiong, P. Current research on ecotoxicity of metal-based nanoparticles: From exposure pathways, ecotoxicological effects to toxicity mechanisms. Front. Public Health 2024, 12, 1390099.
9. Zwozdziak, A.; Sówka, I.; Willak-Janc, E.; Zwozdziak, J.; Kwiecińska, K.; Balińska-Miśkiewicz, W. Influence of PM1 and PM2.5 on lung function parameters in healthy schoolchildren—A panel study. Environ. Sci. Pollut. Res. 2016, 23, 23892–23901.
10. Rahman, M.M.; Khan, S.B.; Jamal, A.; Faisal, M.; Aisiri, A.M. Iron oxide nanoparticles. Nanomaterials 2011, 3, 43–67.
11. Shoudho, K.N.; Uddin, S.; Rumon, M.M.H.; Shakil, M.S. Influence of physicochemical properties of iron oxide nanoparticles on their antibacterial activity. ACS Omega 2024, 9, 33303–33334.
12. Von Der Heyden, B.; Roychoudhury, A.; Myneni, S. Iron-rich nanoparticles in natural aquatic environments. Minerals 2019, 9, 287.
13. Yoshida, A.; Ohata, S.; Moteki, N.; Adachi, K.; Mori, T.; Koike, M.; Takami, A. Abundance and emission flux of the anthropogenic iron oxide aerosols from the East Asian continental outflow. J. Geophys. Res. Atmos. 2018, 123, 11194–11211.

 doi:10.20944/preprints202601.1266.v1

14. Maher, B.A.; González-Maciel, A.; Reynoso-Robles, R.; Torres-Jardón, R.; Calderón-Garcidueñas, L. Iron-rich air pollution nanoparticles: An unrecognised environmental risk factor for myocardial mitochondrial dysfunction and cardiac oxidative stress. Environ. Res. 2020, 188, 109816.
15. Garry, S.; Nesslany, F.; Aliouat, E.; Haguenoer, J.M.; Marzin, D. Hematite (Fe_2O_3) acts by oxidative stress and potentiates benzo[a]pyrene genotoxicity. Mutat. Res. Genet. Toxicol. Environ. Mutagen. 2004, 563, 117–129.
16. Auffan, M.; Decome, L.; Rose, J.; Orsiere, T.; De Meo, M.; Briois, V.; Bottero, J.-Y. In vitro interactions between DMSA-coated maghemite nanoparticles and human fibroblasts: A physicochemical and cyto-genotoxic study. Environ. Sci. Technol. 2006, 40, 4367–4373.
17. Chen, C.; Hu, J.; Shao, D.; Li, J.; Wang, X. Adsorption behavior of multiwall carbon nanotube/iron oxide magnetic composites for Ni(II) and Sr(II). J. Hazard. Mater. 2009, 164, 923–928.
18. Tada, Y.; Yano, N.; Takahashi, H.; Yuzawa, K.; Ando, H.; Kubo, Y.; Nakae, D. Acute phase pulmonary responses to a single intratracheal spray instillation of magnetite (Fe_3O_4) nanoparticles in Fischer 344 rats. J. Toxicol. Pathol. 2012, 25, 233–239.
19. Pease, C.; Rücker, T.; Birk, T. Review of the evidence from epidemiology, toxicology, and lung bioavailability on the carcinogenicity of inhaled iron oxide particulates. Chem. Res. Toxicol. 2016, 29, 237–254.
20. Wu, L.; Wen, W.; Wang, X.; Huang, D.; Cao, J.; Qi, X.; Shen, S. Ultrasmall iron oxide nanoparticles cause significant toxicity by specifically inducing acute oxidative stress to multiple organs. Part. Fibre Toxicol. 2022, 19, 24.
21. Ferraz, F.S.; de PF Dantas, G.; Coimbra, J.L.; López, J.L.; Lacerda, S.M.; Dos Santos, M.L.; Costa, G.M. Effects of superparamagnetic iron oxide nanoparticles (SPIONs) testicular injection on Leydig cell function and sperm production in a murine model. Reprod. Toxicol. 2024, 126, 108584.
22. Imam, S.Z.; Lantz-McPeak, S.M.; Cuevas, E.; Rosas-Hernandez, H.; Liachenko, S.; Zhang, Y.; Gracia, E.; Sarkar, S.; Binienda, Z.K. Iron oxide nanoparticles induce dopaminergic damage: In vitro pathways and in vivo imaging reveal mechanism of neuronal damage. Molecular Neurobiology 2015, 52, 913–926.
23. Patten, K.T.; Valenzuela, A.E.; Wallis, C.; Berg, E.L.; Silverman, J.L.; Bein, K.J.; Lein, P.J. The effects of chronic exposure to ambient traffic-related air pollution on Alzheimer's disease phenotypes in wildtype and genetically predisposed male and female rats. Environmental Health Perspectives 2021, 129, 057005.
24. Abakumov, M.A.; Semkina, A.S.; Skorikov, A.S.; Vishnevskiy, D.A.; Ivanova, A.V.; Mironova, E.; Chekhonin, V.P. Toxicity of iron oxide nanoparticles: Size and coating effects. J. Biochem. Mol. Toxicol. 2018, 32(12), e22225.
25. Caro, C.; Egea-Benavente, D.; Polvillo, R.; Royo, J.L.; Leal, M.P.; García-Martín, M.L. Comprehensive toxicity assessment of PEGylated magnetic nanoparticles for in vivo applications. Colloids Surf. B Biointerfaces 2019, 177, 253–259.
26. Bourgkard, E.; Wild, P.; Courcot, B.; Diss, M.; Ettlinger, J.; Goutet, P.; Moulin, J.-J. Lung cancer mortality and iron oxide exposure in a French steel-producing factory. Occup. Environ. Med. 2009, 66, 175–181.
27. Marchini, T.; Magnani, N.; D'Annunzio, V.; Tasat, D.; Gelpi, R.J.; Alvarez, S.; Evelson, P. Impaired cardiac mitochondrial function and contractile reserve following an acute exposure to environmental particulate matter. Biochim. Biophys. Acta Gen. Subj. 2013, 1830, 2545–2552.
28. Marchini T, Magnani ND, Paz ML, Vanasco V, Tasat D, Maglio DG, et al. Time course of systemic oxidative stress and inflammatory response induced by an acute exposure to residual oil fly ash. Toxicol Appl Pharmacol. 2014;274(2):274–282.
29. Radu M, Din IM, Hermenean A, Cinteză OL, Burlacu R, Ardelean A, et al. Exposure to iron oxide nanoparticles coated with phospholipid-based polymeric micelles induces biochemical and histopathological pulmonary changes in mice. Int J Mol Sci. 2015;16(12):29417–29435.
30. Di Bona KR, Xu Y, Gray M, Fair D, Hayles H, Milad L, et al. Short- and long-term effects of prenatal exposure to iron oxide nanoparticles: Influence of surface charge and dose on developmental and reproductive toxicity. Int J Mol Sci. 2015;16(12):30251–30268.

 doi:10.20944/preprints202601.1266.v1

31. Dos Santos TM, Righetti RF, do Nascimento Camargo L, Leick EA, Fukuzaki S, de Campos EC, et al. Effect of VAChT reduction on lung alterations induced by exposure to iron particles in an asthma model. J Inflamm. 2024;21(1):24.
32. Murthy MK, Khandayataray P, Mohanty CS, Pattanayak R. Investigating the toxic mechanism of iron oxide nanoparticles-induced oxidative stress in tadpole (Duttaphrynus melanostictus): A combined biochemical and molecular study. Environ Toxicol Pharmacol. 2024;107:104432.
33. Pauluhn J. Retrospective analysis of 4-week inhalation studies in rats with focus on fate and pulmonary toxicity of two nanosized aluminum oxyhydroxides (boehmite) and pigment-grade iron oxide (magnetite): The key metric of dose is particle mass and not particle surface area. Toxicology 2009, 259, 140–148.
34. Pauluhn, J. Subchronic inhalation toxicity of iron oxide (magnetite, Fe_3O_4) in rats: Pulmonary toxicity is determined by the particle kinetics typical of poorly soluble particles. J. Appl. Toxicol. 2012, 32, 488–504.
35. Szalay B, Tátrai E, Nyírő G, Vezér T, Dura G. Potential toxic effects of iron oxide nanoparticles in in vivo and in vitro experiments. J Appl Toxicol. 2012;32(6):446–453.
36. Jarockyte G, Daugelaite E, Stasys M, Statkute U, Poderys V, Tseng TC, et al. Accumulation and toxicity of superparamagnetic iron oxide nanoparticles in cells and experimental animals. Int J Mol Sci. 2016;17(8):1193.
37. Matusiak K, Skoczen A, Setkowicz Z, Kubala-Kukus A, Stabrawa I, Ciarach M, et al. The elemental changes occurring in the rat liver after exposure to PEG-coated iron oxide nanoparticles: total reflection X-ray fluorescence (TXRF) spectroscopy study. Nanotoxicology. 2017;11(9–10):1225–1236.
38. Könczöl, M.; Ebeling, S.; Goldenberg, E.; Treude, F.; Gminski, R.; Gieré, R.; Mersch-Sundermann, V. Cytotoxicity and genotoxicity of size-fractionated iron oxide (magnetite) in A549 human lung epithelial cells: Role of ROS, JNK, and NF-κB. Chem. Res. Toxicol. 2011, 24, 1460–1475.
39. Ramesh, V.; Ravichandran, P.; Copeland, C.L.; Gopikrishnan, R.; Biradar, S.; Goornavar, V.; Hall, J.C. Magnetite induces oxidative stress and apoptosis in lung epithelial cells. Mol. Cell. Biochem. 2012, 363, 225–234.
40. Ahamed, M.; Alhadlaq, H.A.; Alam, J.; Majeed, K.; Ali, D.; Alarafi, S. Iron oxide nanoparticle-induced oxidative stress and genotoxicity in human skin epithelial and lung epithelial cell lines. Curr. Pharm. Des. 2013, 19, 6681–6690.
41. Könczöl, M.; Weiss, A.; Stangenberg, E.; Gminski, R.; Garcia-Käufer, M.; Gieré, R.; Mersch-Sundermann, V. Cell-cycle changes and oxidative stress response to magnetite in A549 human lung cells. Chem. Res. Toxicol. 2013, 26, 693–702.
42. Gokduman, K.; Bestepe, F.; Li, L.; Yarmush, M.L.; Usta, O.B. Dose-, treatment- and time-dependent toxicity of superparamagnetic iron oxide nanoparticles on primary rat hepatocytes. Nanomedicine 2018, 13, 1267–1284.
43. Kirschvink JL, Kobayashi-Kirschvink A, Woodford BJ. Magnetite biomineralization in the human brain. Proc Natl Acad Sci U S A. 1992;89(16):7683–7687.
44. Totsuka Y, Ishino K, Kato T, Goto S, Tada Y, Nakae D, et al. Magnetite nanoparticles induce genotoxicity in the lungs of mice via inflammatory response. Nanomaterials. 2014;4(1):175–188.
45. Orel V, Shevchenko A, Romanov A, Tselepi M, Mitrelias T, Barnes CH, et al. Magnetic properties and antitumor effect of nanocomplexes of iron oxide and doxorubicin. Nanomedicine (Lond). 2015;11(1):47–55.
46. Özgür ME, Ulu A, Balcıoğlu S, Özcan I, Köytepe S, Ateş B. The toxicity assessment of iron oxide (Fe_3O_4) nanoparticles on physical and biochemical quality of rainbow trout spermatozoon. Toxics. 2018;6(4):62.
47. Huang, Z.; Xu, B.; Huang, X.; Zhang, Y.; Yu, M.; Han, X.; et al. Metabolomics reveals the role of acetyl-L-carnitine metabolism in γ-Fe_2O_3 nanoparticle-induced embryonic development toxicity via mitochondria damage. Nanotoxicology 2019, 13, 204–220.
48. Kaloyianni, M.; Dimitriadi, A.; Ovezik, M.; Stamkopoulou, D.; Feidantsis, K.; Kastrinaki, G.; et al. Magnetite nanoparticles effects on adverse responses of aquatic and terrestrial animal models. Journal of Hazardous Materials 2020, 383, 121204.
49. Fascineli, M.L.; Cáceres-Vélez, P.R.; Pinheiro, W.O.; Chaves, S.B.; Sousa, M.H.; Peternella, W.S.; et al. Lack of genotoxicity of iron oxide maghemite (γ-Fe_2O_3) and magnetite (Fe_3O_4) nanoparticles to Oreochromis niloticus after acute exposures. Genetics and Molecular Biology 2024, 47(3), e20230330.

 doi:10.20944/preprints202601.1266.v1

50. Silva, A.C.; Dos Santos, A.G.R.; Pieretti, J.C.; Rolim, W.R.; Seabra, A.B.; Ávila, D.S. Iron oxide/silver hybrid nanoparticles impair the cholinergic system and cause reprotoxicity in Caenorhabditis elegans. Food and Chemical Toxicology 2023, 179, 113945.
51. Basso Abraham ALR, Rockenbach de Ávila M, Torres R, Diz VE. Magnetite nanoparticles as a promising non contaminant method to control populations of fruit flies (Diptera: Tephritidae). J Appl Biotechnol Bioeng. 2021;8(4):112–117.
52. Hanini, A.; Schmitt, A.; Kacem, K.; Chau, F.; Ammar, S.; Gavard, J. Evaluation of iron oxide nanoparticle biocompatibility. International Journal of Nanomedicine 2011, 6, 787–794.
53. Safi, M.; Sarrouj, H.; Sandre, O.; Mignet, N.; Berret, J.-F. Interactions between sub-10-nm iron and cerium oxide nanoparticles and 3T3 fibroblasts: The role of the coating and aggregation state. Nanotechnology 2010, 21, 145103.
54. Caldeira, D.F.; Paulini, F.; Silva, R.C.; Azevedo, R.B.D.; Lucci, C.M. In vitro exposure of bull sperm cells to DMSA-coated maghemite nanoparticles does not affect cell functionality or structure. Int. J. Hyperthermia 2018, 34, 415–422.
55. Iversen, N.K.; Frische, S.; Thomsen, K.; Laustsen, C.; Pedersen, M.; Hansen, P.B.; Wang, T. Superparamagnetic iron oxide polyacrylic acid coated γ-Fe_2O_3 nanoparticles do not affect kidney function but cause acute effect on the cardiovascular function in healthy mice. Toxicol. Appl. Pharmacol. 2013, 266, 276–288.
56. Qualhato G, Rocha TL, de Oliveira Lima EC, Silva DM e, Cardoso JR, Grisolia CK, de Sabóia-Morais SMT. Genotoxic and mutagenic assessment of iron oxide (maghemite-γ-Fe_2O_3) nanoparticle in the guppy Poecilia reticulata. Chemosphere 2017, 183, 305–314.
57. Qualhato, G.; de Sabóia-Morais, S.M.T.; Silva, L.D.; Rocha, T.L. Melanomacrophage response and hepatic histopathologic biomarkers in the guppy Poecilia reticulata exposed to iron oxide (maghemite) nanoparticles. Aquat. Toxicol. 2018, 198, 63–72.
58. Lee, Y.; Chun, H.S.; Moon, J.Y.; Choi, J.S.; Park, D.; Lee, Y.C. Correlation of α/γ-Fe_2O_3 nanoparticles with the toxicity of particulate matter originating from subway tunnels in Seoul stations, Korea. J. Hazard. Mater. 2020, 382, 121175.
59. Gürkan, M.; Gürkan, S.E.; Yılmaz, S.; Ateş, M. Comparative toxicity of alpha and gamma iron oxide nanoparticles in rainbow trout: Histopathology, hematology, accumulation, and oxidative stress. Water Air Soil Pollut. 2021, 232, 37.
60. Gonçalves, B.B.; Dias, F.C.; de Souza Trigueiro, N.S.; Marques, E.; Rodrigues, C.C.; Madureira, I.B.; Rocha, T.L. Chronic exposure to iron oxide nanoparticles (γ-Fe_2O_3) induces gonadal histopathology on male guppies (Poecilia reticulata). Environ. Nanotechnol. Monit. Manag. 2021, 16, 100522.
61. Monge-Fuentes, V.; Garcia, M.P.; Tavares, M.C.H.; Valois, C.R.; Lima, E.C.; Teixeira, D.S.; et al. Biodistribution and biocompatibility of DMSA-stabilized maghemite magnetic nanoparticles in nonhuman primates (Cebus spp.). Nanomedicine 2011, 6, 1529–1544.
62. Garry, S.; Nesslany, F.; Aliouat, E.; Haguenoer, J.M.; Marzin, D. Hematite (Fe_2O_3) enhances benzo[a]pyrene genotoxicity in endotracheally treated rat, as determined by comet assay. Mutat. Res. Genet. Toxicol. Environ. Mutagen. 2003, 538, 19–29.
63. Gaharwar, U.S.; Paulraj, R. Iron oxide nanoparticles induced oxidative damage in peripheral blood cells of rat. J. Biomed. Sci. Eng. 2015, 8, 274.
64. Askri, D.; Cunin, V.; Ouni, S.; Béal, D.; Rachidi, W.; Sakly, M.; Sève, M. Effects of iron oxide nanoparticles (γ-Fe_2O_3) on liver, lung and brain proteomes following sub-acute intranasal exposure: A new toxicological assessment in rat model using iTRAQ-based quantitative proteomics. Int. J. Mol. Sci. 2019, 20, 5186.
65. Smital, K.; Niharika, S.; Mansee, T. Sub-acute toxicity assessment of green synthesized hematite nanoparticles (α-Fe_2O_3 NPs) using Wistar rat. Res. J. Biotechnol. 2020, 15, 4.
66. Warshawsky, D.; Reilman, R.; Cheu, J.; Radike, M.; Rice, C. Influence of particle dose on the cytotoxicity of hamster and rat pulmonary alveolar macrophage in vitro. J. Toxicol. Environ. Health A 1994, 42, 407–421.
67. Bhattacharya, K.; Hoffmann, E.; Schins, R.F.; Boertz, J.; Prantl, E.M.; Alink, G.M.; et al. Comparison of micro- and nanoscale Fe^{3+}-containing (hematite) particles for their toxicological properties in human lung cells in vitro. Toxicological Sciences 2012, 126, 173–182.

 doi:10.20944/preprints202601.1266.v1

68. Freyria, F.S.; Bonelli, B.; Tomatis, M.; Ghiazza, M.; Gazzano, E.; Ghigo, D.; et al. Hematite nanoparticles larger than 90 nm show no sign of toxicity in terms of lactate dehydrogenase release, nitric oxide generation, apoptosis, and comet assay in murine alveolar macrophages and human lung epithelial cells. Chemical Research in Toxicology 2012, 25, 850–861.
69. Kalive, M.; Zhang, W.; Chen, Y.; Capco, D.G. Human intestinal epithelial cells exhibit a cellular response indicating a potential toxicity upon exposure to hematite nanoparticles. Cell Biology and Toxicology 2012, 28, 343–368.
70. Faust, J.J.; Zhang, W.; Chen, Y.; Capco, D.G. Alpha-Fe_2O_3 elicits diameter-dependent effects during exposure to an in vitro model of the human placenta. Cell Biology and Toxicology 2014, 30, 31–53.
71. Cardillo, D.; Tehei, M.; Hossain, M.S.; Islam, M.M.; Bogusz, K.; Shi, D.; et al. Synthesis-dependent surface defects and morphology of hematite nanoparticles and their effect on cytotoxicity in vitro. ACS Applied Materials & Interfaces 2016, 8, 5867–5876.
72. Lewis, C.S.; Torres, L.; Miyauchi, J.T.; Rastegar, C.; Patete, J.M.; Smith, J.M.; et al. Absence of cytotoxicity towards microglia of iron oxide (α-Fe_2O_3) nanorhombohedra. Toxicology Research 2016, 5, 836–847.
73. Nations, S.; Wages, M.; Cañas, J.E.; Maul, J.; Theodorakis, C.; Cobb, G.P. Acute effects of Fe_2O_3, TiO_2, ZnO and CuO nanomaterials on Xenopus laevis. Chemosphere 2011, 83, 1053–1061.
74. Oliveira, V.R.; Uriarte, J.J.; Falcones, B.; Jorba, I.; Zin, W.A.; Farré, R.; Almendros, I. Biomechanical response of lung epithelial cells to iron oxide and titanium dioxide nanoparticles. Frontiers in Physiology, 2019, 10, 1047.
75. Rafieepour, A.; Azari, M.R.; Khodagholi, F.; Jaktaji, J.P.; Mehrabi, Y.; Peirovi, H. Interactive toxicity effect of combined exposure to hematite and amorphous silicon dioxide nanoparticles in human A549 cell line. Toxicology and Industrial Health, 2021, 37(5), 289–302.
76. Goadby, K.W. XXIX.—Fibrosis of the lung in iron miners. Journal of the Royal Microscopical Society, 1925, 45(4), 432–437.
77. Lawler, A.B.; Mandel, J.S.; Schuman, L.M.; Lubin, J.H. A retrospective cohort mortality study of iron ore (hematite) miners in Minnesota. Journal of Occupational Medicine, 1985, 27, 507–517.
78. Wang, B.; Feng, W.Y.; Wang, M.; Shi, J.W.; Zhang, F.; Ouyang, H.; et al. Transport of intranasally instilled fine Fe_2O_3 particles into the brain: micro-distribution, chemical states, and histopathological observation. Biological Trace Element Research, 2007, 118(3), 233–243.
79. Rajendran, K.; Pujari, L.; Krishnamoorthy, M.; Sen, S.; Dharmaraj, D.; Karuppiah, K.; Ethiraj, K. Toxicological evaluation of biosynthesised hematite nanoparticles in vivo. Colloids and Surfaces B: Biointerfaces, 2021, 198, 111475.
80. Carleton, H.M. The effects produced by the inhalation of haematite and iron dusts in guinea-pigs. Epidemiol. Infect. 1927, 26, 227–234.
81. Jaiswal, A.K.; Rahman, Q.; Viswanathan, P.N. Enzymatic changes in guinea pig lungs due to haematite dust. Toxicology Letters, 1979, 3(1), 51–54.
82. Das, B.; Khatoon, N.; Srivastava, R.C.; Viswanathan, P.N.; Rahman, Q. Biochemical studies on the toxicity of hematite dust. Environmental Research, 1983, 32(3), 372–381.